Final Progress Report
April 1, 2011.
NIH 1RO1EB004633-01A1
Dendritic Cell Phenotype Upon Contact With Biomaterials
P.I.: Julia E. Babensee

The following is a summary of the progress made on this grant during the funding period August 2005 – December 2010.

Progress:

Specific Aim 1: Demonstrate that biomaterial contact is sufficient for DC maturation into efficient antigen presenting cells (APCs) and T cell stimulators, and that maturation is differentially regulated depending on the type and form of the biomaterial.

Characterization of DC and Macrophage Cultures

The compositions and proportions of the different cell types present in cultures of primary human DCs as compared to macrophages, as derived and used for biomaterial studies, starting from the same human peripheral blood mononuclear cell (PBMC) population, have been characterized as far as cell types present using cytospins and flow cytometry (FC) at different time-points during culture[1].

Phenotype of DCs Upon Biomaterial Contact

Contact of DCs with biomaterials can affect their phenotype to affect functional immunological responses. Maturation of DCs was observed in response to contact with poly(lactic-co-glycolic acid) (PLGA) in forms of microparticles (MPs) or films[2], [3], where the form of the biomaterial (level of maturation greater with MPs than with films) affected the extent of DC maturation and direct contact was required as determined using a transwell assay[4]. Internalization of PLGA MPs was confirmed by treating DCs with fluorescence dye- loaded PLGA MPs, and observing the location of the MPs using confocal microscopy[5]. However, phagocytosis of MPs was not necessary for this maturation effect but biomaterial contact was necessary. To determine this, DCs were treated with MPs of phagocytosable (3 μm) versus non-phagocytosable (20 μm) sizes, of biomaterials with differential effects on DC maturation, keeping the total biomaterial surface area constant[3]. DCs cultured with PLGA (supports DC maturation) or agarose (does not support DC maturation) MPs of the different sizes did not change their expression level of mature DC (mDC) markers, implying that phagocytosis was not the main contributor to the MP-induced DC maturation but exposed biomaterial surface area was[3]. These results were significant since they indicated that direct contact of DCs with a biomaterial surface (e.g., in for form of a film) was sufficient to affect DC maturation and that this was a material effect which had the potential to be controlled.

Demonstration of control over DC phenotype was observed depending on the biomaterial used[2,3]. This differential biomaterial effect on DC maturation and consequent immunological functions was demonstrated by DC treatment with a range of biomaterials commonly used in combination products, tissue engineered constructs and vaccine delivery systems, where desired effects of biomaterials on associated immunological functions are opposite. DCs treated with chitosan or PLGA (agarose to a lesser extent) films induced DC maturation, as compared to control iDCs, similar to LPS-treated mDCs whereas, DCs treated with alginate or hyaluronic acid films decreased their expression levels of these same molecules[2]. PLGA- or chitosan film-treated DCs show dendritic process similar to the mDCs, while the hyaluronic acid (HA)-, alginate-, or agarose film-treated DCs exhibit a rounded morphology similar to iDCs (Figure 1). Mixed lymphocyte reaction (MLR) results showed that DCs treated with PLGA or chitosan films supported T cell proliferation to a higher extent than iDCs whereas, DC treated with HA film, supported lower levels of T cell proliferation than iDCs, actually suppressing T cell

proliferation; DCs cultured on agarose or alginate films were not different from iDCs (Figure 2). Flow cytometric analysis of expression of MHC class II molecules (HLA-DR and HLA-DQ), costimulatory molecules (CD40, CD80, and CD86) was used to support these functional effects. As such, surface molecules of CD80, CD86, CD83, and HLA-DQ, DCs treated with PLGA or chitosan films resulted in significantly higher levels of molecule expression as compared to iDCs. Dendritic cells treated with alginate film resulted in significantly higher levels in molecules of CD83, CD86, and HLA-DQ, as compared to iDCs. However, DCs treated with agarose films did not show significant difference in all surface molecules except CD83 as compared to iDCs. Interestingly, DCs treated with HA film resulted in significantly lower levels of CD40, CD80, CD86, and HLA-DR expression as compared to iDCs. Dendritic cells cultured on PLGA, chitosan, or alginate films released the autocrine stimulatory factor, TNF-α to a level greater than iDCs, while DCs cultured on HA films released less TNF-α than iDCs as determine using ELISAs (Figure 3). Similar results were obtained for release of IL-6. Using the cytometric bead array (CBA) method, a broader profile of cytokines released by biomaterial-treated DCs were assess which included T-helper type 1 (Th 1) cytokines of Interferon (IFN) – γ & IL-12p70 and T-helper type 2 (Th 2) cytokines of IL-10 & IL-4. DCs treated with PLGA or alginate films showed significantly higher levels of IFN– γ release compared to iDCs while other biomaterial treatments showed levels that are not significantly different compared to iDCs. Mature DCs or DCs treated with PLGA showed significantly higher levels of IL-12p70 release compared to iDCs while others did not. Only DCs treated with agarose films showed significantly higher levels of IL-10 release compared to iDCs. However, for IL-4 as the other Th 2 cytokine examined, only agarose films induced levels significantly lower than iDCs.

To examine apoptosis or necrosis of DCs upon treatments with different biomaterial films, Annexin V (apoptosis) and propidium iodide (PI) (necrosis) have been stained with DCs treated with different biomaterial films and then, intensities of each staining have been measured using the FC. Mature DCs, DCs treated with PLGA, chitosan, alginate, or HA films showed significantly higher levels of Annexin V expression compared to iDCs while DCs treated with agarose film showed expression level which is not significantly different with iDCs. For PI expressions, only DCs treated with alginate films induced significantly higher levels compared to iDCs.

Another functional measure of DC phenotype is their endocytic activity. Immature DCs are highly phagocytic but lose this ability with maturation mirroring their shift in receptor expression with high levels of phagocytic receptors on iDCs and high levels of MHC and co-stimulatory molecules on mDCs. Phagocytic uptake of FITC-dextran (40,000 MW) molecules by differentially biomaterial treated DCs, as determined by FC, demonstrated high endocytic ability by iDCs while mDCs, DCs treated with PLGA or chitosan films exhibited less ability compared to the iDCs. However, DCs treated with HA films unexpectedly exhibited less ability similar to that of DCs treated with PLGA films which is contrary its phenotype as determined by other assays. This endocytic activity was correlated with expression levels of surface molecules related to the endocytic or migration of DCs, CD32 (Fc-gamma receptor type II), CD206 (mannose receptor), and CD44 [receptors for hyaluronan component in ECM for DC migrations] determined using FC. Supporting these results, DCs treated agarose film expressed CD32 or CD206 in levels higher than or similar to iDCs, respectively, while mDCs or all other biomaterial treatments showed significantly lower levels than iDCs. Even though CD44 has been well known for high expressions on DCs against the HA components of small fragment in soluble forms, HA films in this study exhibited lowest level of expression among all biomaterial films. This indicates that cross-linked & insolublized HA films in this study might induce no or less expression of CD44 as compared to the control of iDCs. Interestingly, CD44 expression levels of controls and treatments shows patterns very similar to that of surface marker expressions (CD80 & CD86) or MLRs for DC maturations upon treatments with different biomaterials.

High Throughput Methodology to Assess DC Phenotype

The assessment of DC maturation in response to biomaterials generally includes DC culture in the presence of biomaterials in a 6-well plate format and the quantification of surface marker expression by conventional flow cytometry (Figure 4). However, such method is time-consuming and is suitable for the evaluation of only a limited number of biomaterials. As a result, a high throughput (HTP) methodology was developed desired to study DC phenotype upon the contact with arrays of biomaterials[6]. This method uses filter plate for rapidly washing of the cell samples without any cell loss and fluorescence detection *in situ* showed promising results for the HTP assay. Briefly, after treatment with biomaterials, the DCs are transferred to a black 96-well filter plate, fixed, and stained with anti-CD86-PE and anti-DC-SIGN-FITC antibodies. The ratio of CD86-PE/DC-SIGN-FITC, or "maturation factor", is a DC number-independent parameter to represent DC maturation. In addition, the cell culture supernatants could be collected easily through the bottom of the filter membranes from the individual wells. The supernatants could be immediately used for the assessment of biomaterial-induced cytotoxicity or stored at -80°C for multiplex cytokine analysis. Figure 4 illustrates the experimental scheme of the conventional assessment of DC maturation as well as the filter plate-based HTP screening methodology. The differential effects of PLGA or agarose on resultant DC phenotype have also been demonstrated in a scaled-down 96-well filter plate high throughput (HTP) format to analyze DC maturation (Figure 5). This technique has been further scaled down to a 384-well plate with consistent results (Figure 6).

Biomaterial-Treated DC Direct Autologous T Cell Phenotype and Polarization

As a read-out for the ability of biomaterial-treated DCs to direct T cell responses, DCs were treated with the different biomaterial films and their functional impacts in regulating autologous T cell phenotype and polarization were assessed. Biomaterial-treated DC-directed autologous T cell phenotype and polarization were assessed by examining expression of T cell markers [CD4 (T helper), CD8 (cytotoxic T cell)] and activation markers [CD25 (regulatory T cell marker) and CD69] and differential cytokine profiles. Differentially biomaterial-treated DCs' ability to direct autologous T cell mediated immunity was demonstrated *in vitro*. DCs treated with agarose induced significantly higher expression of CD4+CD25+ T cells (Figure 7a) of which this population (Figure 7c) were FoxP3+ (Figure 7c) on co-cultured autologous T cells indicating T_{reg} induction and release of the immunosuppressive cytokine, IL-10, at higher levels than iDCs (Figure 7b). In contrast, DC treated with PLGA induced release of IFN-γ at higher levels in the DC-T co-culture system, than iDCs (Figure 7b). Clearly the results show that the phenotype of autologous T cells and polarization of their cytokine profiles can be differentially modulated in co-cultures with DC treated with different biomaterials. This is a powerful non-pharmacological immunotherapy tool to be further explored and its applications developed.

Phenotype of DCs Upon Treatment with Biomaterial Scaffolds

Since in tissue engineering, these materials would be used in a three dimensional, porous scaffold form, we have examined the relevance of our film studies by treating DCs with biomaterials which have shown differential levels of DC maturation now in a 3D scaffold form. Differential levels of DC maturation were observed on porous PLGA scaffolds prepared by solvent casting and particulate leaching[7] and porous agarose scaffolds prepared by inverted colloidal crystal templating[8] consistent with their effects in film form on DC maturation. DCs seeded on PLGA films exhibited dendritic processes of an mDC morphology while DCs seeded on agarose scaffolds were rounded of an iDC morphology (Figure 8). Treatment of DCs with porous PLGA scaffolds resulted in significantly higher levels of expression of CD40, CD80, CD86, and HLA-DR as compared to iDCs, while treatment with porous agarose scaffolds were less than or similar to iDCs for all molecules examined. Furthermore, DCs treated with PLGA scaffolds showed allostimulatory capacities significantly higher than iDCs whereas, DC treated

with agarose scaffolds showed levels similar to iDCs (Figure 8). For measurements of apoptosis and necrosis of DCs upon treatments with scaffolds, DCs treated with PLGA scaffolds exhibited significantly higher levels compared to controls or DCs treated with agarose scaffolds for both of Annexin V and PI. Overall, DCs treated with PLGA or agarose 3-D porous scaffolds showed DC maturation or apoptosis/necrosis patterns very similar to those of DCs treated with PLGA or agarose 2-D films.

Principal Component Analysis (PCA) Suggested DC Phenotype-Material Property Relationships for pMA and terpolymer Combinatorial Libraries

Our studies have revealed that different biomaterials induce different levels of DC maturation or even suppress it. Studies with these commonly used biomaterials for combination products were very important to assess their effect on DC maturation, to note biomaterial differences and to establish the biomaterial effect on DC phenotype as a novel biocompatibility design and selection criteria for biomaterials to be used in combination products where immunological responses may be of consequence. However, with these commonly used biomaterials in combination products, it is unclear which material properties have caused such differential effects. Thus we undertook studies in collaboration with Dr. Joachim Kohn's laboratory to assess DC responses to combinatorial libraries/arrays with graded material properties using a high throughput system we have developed.

To draw relationships between biomaterial properties and DC phenotype, two combinatorial libraries of polymers, with graded variations in their well-characterized properties, were used to treat DCs with assessment of resultant phenotypic outcomes and data analysis using principal component analysis (PCA).

The libraries used were one of polymethacrylate (pMA) and another of terpolymer (composed of HEMA, EHA, TEGMA, and/or NIPAAM as well as GMA). Polymers were solvent cast into the wells of 96-well polypropylene plates and used to treat human blood derived DCs for 24h using a high throughput (HTP) method[6], in which DC maturation was measured by the metric CD86/DC-SIGN using immunostaining. Supernatants were collected for cytotoxicity analysis and cytokine profiling. Endotoxin contents of all polymers were < 0.3 EU/mL and non-cytotoxic to DCs.

The polymers used in the studies were characterized for glass transition temperature (T_g), molecular weight (Mw), contact angle (θ), surface roughness (Sa), surface area, and surface chemical composition by XPS for both polymer libraries. For the terpolymer library, wet modulus (WM) and surface mass spectral information by ToF-SIMS were additionally characterized. The phenotype variables (n=6 independent donors) and material property variables were analyzed by PCA to extract latent relationships among the variables.

This collaborative work is the first feasibility demonstration of a new HTP testbed that can be used to explore a wide range of cell-material interactions. For the pMA (Figure 9 A-D) and terpolymer (Figure 9 E-H) libraries, the DC maturation trend, represented by the metric CD86/DC-SIGN ratio, as a function of polymer treatment, was similar to the trend of pro-inflammatory cytokines (e.g. TNF-α) and chemokines (e.g. IL-8). In contrast, the trend of DC maturation was inverse to the trend of IL-16 (pleiotropic cytokine) production in the pMA library but similar to that in the terpolymer library, with pHEMA inducing highest levels of IL-16.

Effects of certain material properties were different depending on the library. For example, in the pMA library (Figure 10A), PCA suggested that T_g was not important in determining DC phenotype, whereas in the terpolymer library (Figure 10B), increase in T_g, as well as WM, were associated with DC maturation. In contrast, for both libraries, surface carbon was associated with increased DC maturation, while surface oxygen was accompanied reduced DC maturation (Figure 10). Such differences may be interpreted by three possible explanations: 1) material properties of distinct types of polymers might exert differential effects on DCs, and that the DC phenotype-material property relationships may need to be characterized for a

specific type of polymers; 2) the terpolymer library was a better controlled system with the goal to adjust only one material property at a time, so such system may allow for better delineation of material property-DC phenotype relationships; 3) these contradictory results might also indicate that properties such as T_g is not a determinant on DC phenotype. Conversely, a material property that had a consistent effect on DC phenotype was surface chemistry; hence current work to obtain surface mass spectral signature for the terpolymer library to predict DC phenotype.

DC Phenotype Upon Treatment with Well-Characterized and Defined Titanium (Ti) Surfaces

The DC responses to well-characterized and defined titanium (Ti) surfaces were assessed and PCA was used to correlate material properties and DC phenotype[9]. The set of titanium (Ti) surfaces, included pretreatment (PT), sand-blasted and acid-etched (SLA) and modified SLA (modSLA) with well-defined roughness, surface energy, and surface chemistry. DCs expressed higher CD86 after treatment with PT or SLA, but the DCs treated with modSLA expressed CD86 at a level similar to iDCs; however, no difference was found between PT and SLA treatments for CD86 expression in DCs (Figure 11). Interestingly, DCs treated with modSLA substrates were still able to fully mature in response to LPS (data not shown). Furthermore, SEM micrographs showed that DCs treated with PT or SLA substrates exhibited more dendritic processes associated with mDCs, while modSLA treated DCs were rounded, which is a morphology associated with iDCs (Figure 12A – C). After a 24 h exposure to the Ti substrates, the percent DC recovery (recovered DCs / plated DCs) was similar for both the loosely- or non-adherent and adherent fractions of cells (Figure 13). Percent DC recovery from the LPS-treated culture was higher than from DCs cultured on TCPS or treated with modSLA. Furthermore, the percent adherent DCs (adherent DCs / recovered DCs) was not different among the different Ti substrates, but percent adherent DCs on TCPS was lower than on any of the substrates (Figure 13). Low magnification (150x) SEM images of cells remaining on the substrates after non-adherent cells were washed away, indicate that the number of adherent DCs on these Ti substrates was similar (Figure 12D-F). Multiplex cytokine analysis showed that production of factors was substrate-dependent. PT surfaces induced higher levels of IL-1ra production by DCs compared to the negative control or modSLA substrates. As expected, LPS-treated DCs released higher amounts of IL-1ra compared to the iDC control (Figure 14). Although some trends in the production of TNF-α, IL-10 and MIP-1α were observed among the Ti substrates, the differences were not statistically significant. LPS-treated DCs produced higher TNF-α, IL-10 and MIP-1α relative to any other treatments. The analysis of a wider array of cytokines and chemokines (Figure 15) indicated that SLA surfaces induced higher levels of IL-16 production by DCs compared to modSLA or TCPS, while PT-treated DCs released higher amounts of MCP-1 relative to the TCPS control and to a level not different from LPS-treated DCs. LPS induced increased production of MCP-1 compared to TCPS, SLA or modSLA. Furthermore, all of these three Ti substrates induced minute productions of pro-inflammatory cytokines (IL-1β, IL-12p70 and IL-18) compared to LPS treatment of DCs. Although the substrate-induced production of IL-8 by DCs followed the trend of SLA > PT > modSLA, the differences were not significant. In addition, LPS-treated DCs released higher IL-8 compared to TCPS or any substrate treatment. All Ti substrates induced IL-15 production by DCs at levels below detection limit (data not shown). Trends of TNF-α, IL-1ra, IL-10 and MIP-1α production were similar to Figure 14. Because SLA and modSLA essentially have the same surface roughness but have very different water-air contact angles (138.3° vs 0°), this result suggests that hydrophilicity of a surface is an important property that modulates DC maturation.

Together, modSLA induced the least mature DC phenotype. Notably, DCs treated with modSLA released the least amount of chemokines to attract other innate cell types, which may reduce the intensity of the innate immune responses. The results supported that modSLA may have clinical benefits in suppressing inflammation while enhancing bone formation. In addition,

because used and cleaned Ti surfaces induced different response profile, these surfaces may not be used to replace brand-new materials and should be used with caution.

The first PCA analysis confirmed experimental data that extents of DC maturation were Ti substrate-dependent (Figure 16). The data set could be modeled using two PCs, which were able to represent 95.9% of the data. The PCA biplot indicated that modSLA clustered with TCPS for its effects on DC responses, while SLA and PT formed another cluster that was closer to the LPS treatment. As expected, LPS induced drastic phenotypic changes in DCs and was strongly associated with the phenotype variables along the far end of the first PC (PC1) (thick black dotted ellipse in Figure 16). Consistent with the experimental result, PT treatment was more strongly associated with IL-1ra production than the other two Ti treatments as shown along the second PC (PC2) (thin black dotted ellipse in Figure 16). Overall, SLA induced higher DC maturation as compared to PT because it was situated closer to the phenotype variables along PC1, while modSLA-treated DCs were negatively associated with the phenotype variables (Figure 16).

The second PCA analysis suggested DC phenotype–Ti material property relationships (Figure 17). The data set could be modeled by three PCs capturing a total of 74.4% of information. The first 2 PCs (PC1 and PC2) were able to represent 59% of data variance. Instead of a biplot, the score plot and loadings plot are shown for clarity. The relative locations of PT, SLA and modSLA in the score plot were consistent with the PCA biplot shown in Figure 16. In addition, in the loadings plot, CD86 expression and surface roughness (R_a) primarily contributed to PC1 and PC2, respectively, suggesting that roughness had little effect on CD86 expression, which was consistent with the experimental result. Furthermore, air-water contact angle (Theta), surface %C and %O were more associated with an mDC phenotype due to their clustering with phenotype variables that were up-regulated upon DC maturation (blue dotted ellipse in Figure 17). Higher values of these surface characteristics were associated with PT and SLA substrates, which were shown to promote DC maturation. In contrast, surface %O and %Ti, which were higher on modSLA substrates, were on the opposite side of the phenotype variables (black dotted ellipse in Figure 17), indicating that these surface properties tended to promote an iDC phenotype. Interestingly, air-water contact angle was strongly associated with IL-10 production, and %C and %N were similar in their effects on DC phenotype. Information from plots of PC1 and PC3 provided similar conclusions as PC1 and PC2, while plots formed by PC2 and PC3 resulted in meaningless covariations (data not shown).

Specific Aim 2: Evaluate the mechanism of DC maturation by biomaterials, particularly the receptors involved focusing on Toll-like receptors (TLRs) of the innate immune system.

Role of Phagocytosis and Biomaterial Surface Area on DC Maturation

As DC maturation effects were observed upon treatment with PLGA, mechanisms and receptors involved in PLGA- induced DC maturation were further evaluated. We have previously observed that MP form of DCs induced higher maturation than did film form, suggesting that phagocytosis of MPs may induce higher levels of DC maturation[4]. Internalization of PLGA MPs was confirmed by treating DCs with fluorescence dye- loaded PLGA MPs, and observing the location of the MPs using confocal microscopy[5]. To further probe the effect of phagocytosis or simply biomaterial contact on the extent of DC maturation, PLGA microparticles of phagocytosable (3 μm) versus non-phagocytosable (20 μm) sizes were used to treat DCs, keeping the total biomaterial surface area constant. DCs cultured with PLGA or agarose MPs of the different sizes did not change their expression level of mDC markers, implying that phagocytosis was not the main contributor to the MP-induced DC maturation but exposed biomaterial surface area was[3].

Role of TLRs on Biomaterial-Induced DC Maturation

Toll-like receptors (particularly TLR4 but also TLR2) have been implicated in the recognition of many endogenous ligands such as high mobility group box (HMGB)1, HA fragments and HSP60. Hence, due to the wide variety of putative 'danger signal' ligands which may be generated in response to construct implantation or associated with a biomaterial implant, the role of TLR4 in mediating DC recognition of and response to biomaterials was assessed, along with other PRRs. One approach to assess the roles of receptors known to be involved in DC maturation/signaling and phagocytosis, specifically, CD14, CD36, CD51, DC-SIGN, mannose receptor, TLR2, and TLR4, was to use blocking antibodies against these receptors with evaluation of PLGA-induced human DC maturation and uptake of PLGA MPs. However, results from *in vitro* blocking studies of human DCs were not encouraging, with increased DC maturation (by FC and TNF-α release) due to pretreatment of antibodies alone, without maturation stimulants, and the lack of blocking effect on LPS-induced maturation.

The second approach to assess the role of CD14 and TLR4 in the PLGA- induced DC maturation was to use DCs derived from the BM of commercially available murine models of hyporesponsive LPS-dependent signaling, mice deficient in TLR4. For this purpose, we established our ability to derive murine $CD11c^+$ DCs in culture and demonstrate their robust maturation responsiveness to PLGA MPs and films, as expected based on human DC results, using BM from C57BL/6 mice[10]. To assess the role of TLR4 in PLGA-induced DC maturation, maturation in response to PLGA MPs or films was assessed for loosely-adherent $CD11c^+$ DCs derived from BM harvested from TLR4 deficient mice C57BL/10ScNJ ($TLR4^-$) as compared to the control C57BL/10ScSnJ ($TLR4^+$) mice. DCs derived from C57BL/10ScSnJ ($TLR4^+$) [but not C57BL/10ScNJ ($TLR4^-$)] mice treated with ultrapure-LPS (*Invivogen*) showed signs of DC maturation with increases in expression of $I\text{-}A^b$, CD80 and CD86 (Figure 18). Treatment of DCs from C57BL/10ScSnJ ($TLR4^+$) mice with PLGA biomaterial films slightly increased the expression of CD86 (a sign of DC maturation) but not in the DCs from C57BL/10ScNJ ($TLR4^-$) mice (Figure 18). Therefore, it is possible that TLR4 plays a role in biomaterial-induced DC maturation. However, the C57BL/10ScSnJ ($TLR4^+$) DCs response to the ultrapure LPS treatment was not as robust as previously seen with DCs derived from C57BL/6 mice. Therefore, another appropriate $TLR4^+$ control strain (C57BL/10J) was used as a source of DCs to examine if they would be more responsive to LPS or biomaterial treatments. However, DCs derived from this TLR4+ control strain, C57BL/10J, were even less responsive to PLGA film treatment due to the loosely-adherent untreated iDC controls showing high levels of maturation ($I\text{-}A^b$, CD86 expression) or pre-activation.

To identify at what step of the murine DC culture this pre-activation of the loosely-adherent iDCs was occurring, a characterization was performed for DCs derived from either C57BL/6 or C57BL/10ScSnJ mice in which the purity of the DC culture was analyzed using a wide variety of markers for various cell populations and DC markers of maturation at critical time points for both the loosely-adherent and adherent DC populations. DC cultures from both strains exhibited similar initial presence of B cells and granulocytes but by day 6 of culture these populations were minimal and following $CD11c^+$ isolation were completely absent. Interestingly, loosely-adherent DCs were found to be of a more mature phenotype while the adherent DCs were of an immature phenotype. Prior to plating DCs for treatment, DCs displayed a double-positive population of $I\text{-}A^b$ (low and high). After plating for 24hr treatment, the population expressing lower $I\text{-}A^b$ levels became adherent while the population expressing higher $I\text{-}A^b$ levels was loosely-adherent. The postulation that the adherent DCs were less activated than the loosely-adherent DCs was further supported by their response to ultrapure-LPS treatment. Adherent DCs from C57BL/6 or C57BL/10ScSnJ mice exhibited greater increases in expression of $I\text{-}A^b$ and CD86 in response to ultrapure-LPS than loosely-adherent DCs (Figure 19). This enhanced responsiveness of adherent DCs to stimuli was borne out in a subsequent experiment in which the responsiveness of adherent DCs derived from C57BL/6 mice was confirmed with increases

in I-A^b and CD86 following LPS or PLGA film treatments, more so than the loosely-adherent fraction. This validates our attempt to use adherent DCs as a less pre-activated form of DCs.

After finding adherent DCs more responsive, the role of TLR4 in biomaterial-induced maturation was examined by analyzing both the loosely-adherent and adherent DC fractions. BM DCs were cultured from C57BL/10J ($TLR4^+$) or C57BL/10ScNJ ($TLR4^-$) strain as previously described and treated as iDC with ultrapure-LPS or treated with biomaterials, PLGA films or MPs. Unlike adherent DCs from C57BL/6J mice, adherent DCs from the $TLR4^+$ strain C57BL/10J were unresponsive to PLGA films across all markers, with exception of an MHCII molecule (I-A^b). The adherent DCs from C57BL/10J mice were more responsive to ultrapure-LPS than the loosely adherent DCs as anticipated. However, the prominent maturation-inducing effects of biomaterial treatment seemed to be absent in DCs from C57BL/10J mice.

In summary, adherent BM-derived murine DCs were more responsive to maturation stimuli than loosely-adherent DCs. However, the maturation inducing stimulus of PLGA films dramatically seen with adherent DCs from C57BL/6J was not found with the appropriate $TLR4^+$ strain for C57BL/10ScNJ ($TLR4^-$) mice. Hence, an appropriate $TLR4^+$ control strain was not identified for these experiments in which the role of TLR4 in mediating biomaterial-induced DC maturation could be elucidated. Furthermore, for all of these maturation effects by LPS or biomaterials, the human DC culture system was consistently more robust, hence it will form the basis for the experiments described in this proposal to assess the role of PRRs, including TLRs, in the DC recognition and response to biomaterials.

The third approach which was used to assess the role of TLRs in the DC response to biomaterials was to assess a key consequence of these receptors' ligation which is the activation of the transcription factors, NF-kB and AP-1. Dendritic cells treated with agarose or PLGA films showed levels of activation of NF-kB family members, as determined by ELISAs, in between those of iDCs and LPS- matured DCs[3]. However, DCs treated with agarose showed higher activation levels of all members of NF-kB family assessed, as compared to PLGA-treated DCs[3]. No significant difference in levels of p50 were observed for the DCs treated with the all biomaterial films as compared to iDCs, except DC treated with alginate for 5 hours or that treated with agarose for 24 hours which showed significantly lower or higher levels compared to iDCs, respectively. The levels of p50 were undetectable from DCs treated with the HA films. Assessing the effect of time, the levels of p50 increased from 5 to 24 hours for mDCs or DCs treated with alginate film. We have not yet reconciled this difference between the other readouts of DC maturation and NF-kB activation.

In further studies, to isolate the role TLR4 may play in DC recognition of biomaterials, a model cell line, HEK-293 cells stably transfected with TLR4, MD2 and CD14 (*Invivogen*) (TLR4-expressing HEK-293 cells), were treated with LPS, PLGA films or agarose films and analyzed for NF-κB and AP-1 activation and IL-8 secretion. It was found that NF-κB activation (across all family members at both 5 and 24hr time points) and IL-8 secretion only occurred in the LPS-treated cells, not PLGA or agarose films-treated cells. However, most AP-1 family members were activated by LPS, PLGA or agarose films at the 24-hr time point. These results indicated that DCs may use mechanisms analogous to pathogen recognition to respond to biomaterials (e.g. TLRs). Furthermore, this is the first indication of a means by which biomaterials may be different from bacteria in their activation of inflammatory cells, primarily through their signaling effects through TLR4. However, the TLR4 dependence of this LPS-induced NF-kB, AP-1 activation and IL-8 secretion could not be established using TLR4 blocking antibody likely due to high expression levels of this receptor by the tranfected cells.

As an alternative TLR4-signaling blocking strategy, a MyD88-silenced cell line was established using a MyD88-specific short-hairpin RNA (shRNA) expressing plasmid to block/inhibit downstream signaling from TLR4 (MyD88 propagates signal from all TLRs except TLR3). MyD88-silencing was confirmed by immunoblotting where MyD88-silenced cells

showed significant reduction in MyD88 expression. Un-silenced (control) and MyD88-silenced TLR4-expressing HEK-293 cells were tested for NF-κB (p65 subunit only) and AP-1 (c-Jun subunit only) activation upon treatment with LPS, PLGA films or agarose films for 24 hrs. Control cells exhibited increases in NF-κB activation in response to LPS (though not statistically significant) but not PLGA or agarose films. However, MyD88-silenced cells showed similar NF-κB activation in response to LPS indicating that TLR4-signaling had not been inhibited. Also showing lack of inhibition, MyD88-silenced cells showed significant increase in AP-1 activation (c-Jun) in response to agarose films showing that MyD88-silenced TLR4-expressing cells (to an extent) still responded to agarose films. Control cells did not show any significant increase in AP-1 activation in response to LPS, PLGA or agarose films. As another control, LPS, PLGA or agarose film treatments did not induce activation of NF-κB (p65) in 293-null cells (wild type). However, PLGA or agarose film treatments did induce activation of AP-1 (c-Jun) in 293-null cells. This implies that biomaterial-induced AP-1 activation was not dependent on the over-expression of TLR4 in this cell line.

A consequence of AP-1 activation is an effect on cell survival. To examine whether the biomaterial-induced AP-1 activation seen here was yielding increased apoptosis, we treated the three cell lines (293-null, TLR4-expressing HEK293 cells and MyD88-silenced TLR4-expressing HEK293 cells) as before with PLGA or agarose films for 24 hrs. Cytosolic extracts were harvested and examined for early markers of apoptosis (activated caspase 8 and caspase 3) by a fluorometric technique (*BioSource*). Across the cell lines, agarose treatment induced significant reductions in activated caspase 8 presence than from TCPS controls possibly indicating a survival mechanism. For LPS or PLGA treatment, MyD88-silenced cells showed a significant increase in activated caspase 8 presence in cytosol as compared to controls. Activated caspase 8 cleaves the pro-form of caspase 3 into its activated form which then continues the signaling cascade of apoptosis. Caspase 3 activity was found to match caspase 8 activity for the MyD88-silenced cell line treated with LPS or PLGA and the TLR4-expressing HEK-293 cells treated with agarose.

Role of TLRs in the Acute and Chronic Inflammatory Response to an Implanted Biomaterial

Using an established TLR4-deficient mouse strain, C57BL/10ScN[11], which possesses a complete deletion of the *tlr4* gene, along with an appropriate wild-type control strain (C57BL/10) as recipients of biomaterial implants, the role of TLR4 in the host response to a biomaterial implant was examined[12]. To study the role of TLR4/DAMP interactions in the acute inflammatory response to biomaterials, PET discs were implanted IP for 16hr in $TLR4^-$ or $TLR4^+$ mice and total leukocyte concentrations and differential leukocyte profiles were analyzed in IP lavages and adherent cells harvested from the discs. Sham surgeries and naïve mice were used as controls to isolate the role TLR4/DAMP interaction plays in the recruitment of leukocytes due to the biomaterial itself. The TLR4 dependence of the fibrous capsule formation was assessed following 2 weeks of PET disc implantation subcutaneously in $TLR4^-$ or $TLR4^+$ mice.

Total leukocyte concentrations were determined in IP lavages collected from $TLR4^+$ or $TLR4^-$ mice receiving a PET disc implant, sham surgery or in the naïve control group (Figure 20). Implantation of a PET disc induced recruitment of leukocytes into the peritoneal cavity of $TLR4^-$ mice with higher total leukocyte concentrations as compared to that of the respective naïve mice. This trend was also present upon PET disc implantation into $TLR4^+$ mice but was not found to be statistically significant. Sham surgery induced leukocyte recruitment into the peritoneal cavity of either mouse strain to levels which were between those found for naïve or implant groups of either mouse strain, though not-statistically different from either group (Figure 20).

The differential leukocyte profiles in IP lavages for $TLR4^+$ or $TLR4^-$ mice were determined and found to be similar for both mouse strains for the various treatment groups (Figure 21). The majority of leukocytes in the peritoneal cavity at 16hr were neutrophils for both mouse strains regardless of treatment; however, there was a significantly lower fraction of neutrophils in naïve $TLR4^-$ than all $TLR4^+$ treatments (Figure 21A). $TLR4^-$ mice tended to have a slightly higher fraction of monocyte/macrophage than $TLR4^+$ mice (Figure 21B); however, no significant differences were found between implant groups of the two strains. Eosinophil and lymphocyte fractions from both strains were found to be similar (Figure 21C, 21D, respectively). To examine if a TLR4 deficiency affected circulating leukocyte concentrations, which would certainly have affected recruitment into the IP space, total circulating leukocyte concentrations were determined in lysed whole blood obtained from cardiac punctures. No differences were found across all treatments (data not shown) for both $TLR4^+$ and $TLR4^-$ mice.

As a potent pro-inflammatory cytokine often produced upon TLR4 signaling, TNF-α controls numerous cellular actions in the acute inflammatory response. The concentration of TNF-α in peritoneal cavity was determined to assess if it was induced in a TLR4-dependent manner following biomaterial implantation for 16hr. TNF-α was only significantly detected in the peritoneal cavity upon implantation of a PET disc since little to no TNF-α was detected in IP lavages of sham or naïve groups from both $TLR4^+$ and $TLR4^-$ mice (Figure 22). However, this response was found to be TLR4-independent as both strains elicited similar production of the cytokine upon PET disc implantation.

The role of TLR4 in controlling the adherent leukocyte profile on the IP implanted PET disc was assessed by determining the total number and differential profiles of leukocytes harvested by trypsinization from discs. The total numbers of leukocytes recovered as adherent to the biomaterial were similar in $TLR4^+$ and $TLR4^-$ mice (Figure 23A). However, the differential leukocyte profiles recovered from the surface of the material were distinct between strains (Figure 23B). Implants in $TLR4^+$ mice possessed equivalent fractions of harvested adherent neutrophils and monocyte/macrophages while implants in $TLR4^-$ mice had significantly higher fractions of adherent neutrophils than monocyte/macrophages (Figure 23B). Furthermore, both of these fractions were significantly different between the two strains (Figure 23B).

To examine whether TLR4 presence affected the fibrous encapsulation of an implanted biomaterial, PET discs were implanted SC in $TLR4^+$ or $TLR4^-$ for 2 weeks and the resultant thicknesses assessed in histological sections. Tissue surrounding the implants was stained with Van Gieson to highlight the collagen content of the capsule. $TLR4^+$ and $TLR4^-$ mice displayed no noticeable differences in collagen content at the implant interfaces. Both strains elicited a strong tissue reaction (Figure 24A-D) as well as a thick fibrous capsule on the dermal side as opposed to the muscle, which was thin (Figure 24). The capsule on the dermal side was determined to be 16 ± 4 μm for $TLR4^+$ mice and 18 ± 2 μm for $TLR4^-$ mice while the capsule adjacent to muscle was 8 ± 2 μm for $TLR4^+$ mice and 9 ± 2 μm for $TLR4^-$ mice. There were no differences in the thicknesses of the fibrous capsules on either side between the two strains.

Gene Expression Patterns Of TLRs/Inflammatory Molecules Or Chemokine Receptors/Integrins, In The Response Of DCs To Biomaterials

To probe gene expression patterns of TLRs/inflammatory molecules or chemokine receptors/integrins, in the response of DCs to biomaterials, the expression of relevant genes was probed using either the TLR-focused RT^2 Profiler Array or a custom designed qRT-PCR Array[13], respectively, with appropriate validation for the latter. Hierarchical clustering of TLR/inflammatory related genes showed that DCs treated with PLGA films clustered tightly with

the LPS-treated mature DCs while agarose treated DCs clustered tightly with iDCs (Figure 25a). This result lends further credence to the differential effects of PLGA and agarose films on DC phenotype as described above. However, in contrast, hierarchical clustering of chemokine receptor/integrin genes showed that DCs treated with PLGA films induced a distinct mature phenotype which differed from that induced by LPS treatment (Figure 25b). In fact, the expression pattern of these genes resembled that of iDC and DCs treated with agarose films rather than mDCs. In summary, these arrays can provide valuable insight as overall view gene expression patterns with different stimuli and clustering. However the contradiction in hierarchical clustering for these two arrays for the treatment groups indicates that there is a caveat with these arrays in that there is pre-selection of genes available for clustering. This can affect the clustering results between treatment groups. Hence, these arrays, while providing a more global view of DC responses to stimuli by assessing expression of multiple genes, also have their limitations. Furthermore, the feasibility of only testing a limited number of time points (here 24 hrs) of stimulation may not be optimal for observing peaks of expression for all genes.

Involvement of Integrins in PLGA- induced DC maturation

The role of β integrins in DC adhesion and responses to PLGA was assessed[14]. To initially investigate the level of DC adhesion to biomaterials, the adherent cell fraction on either TCPS or PLGA surfaces was imaged using microscopy. Adherent cells on both substrates were fixed and stained with DC surface marker (DC-SIGN) to assure the specific assessment of DCs. As shown in Figure 1, DCs present on TCPS surface mostly appeared round in morphology (Figure 26A). This is in contrast to DCs treated with PLGA films which showed more cellular adhesion to the surface and nearly all DCs exhibited dendrites reaching over 100μm (Figure 26B). On both substrates, each adherent cell was DC-SIGN$^+$ (a human DC marker) (Figure 26 C,D) while being negative CD19 (B cells), a contaminating cell population in this culture system (data not shown).

In order to pinpoint adhesion molecules potentially responsible for the recognition of biomaterials by DCs, a gene expression analysis was undertaken to determine how DC adhesion and/or DC activation influences integrin and other adhesion molecule mRNA expression. Dendritic cells were cultured on TCPS as a negative control for iDC, treated with PLGA or agarose films, or cultured on TCPS and stimulated with ultrapure-LPS as a positive control for mDCs. As shown in Figure 25b, DCs cultured on TCPS (iDC) or treated with agarose films showed similar gene expression patterns (qualitative analysis as seen through tight cluster) across all adhesion-related molecules investigated. In contrast, the activating treatments of PLGA films or ultrapure-LPS (mDC) clustered together, though to a lesser extent than agarose and TCPS (Figure 25b). Adhesion-related signaling molecules (such as FAK) were down-regulated in response to ultrapure-LPS but unaffected upon PLGA treatment. There was a noted difference in the integrin gene expression pattern to PLGA and ultrapure-LPS. While ultrapure-LPS induced down-regulation of integrin subunits (α_M, β_1, β_2, α_X, and α_5), PLGA treatment induced an up-regulation of these molecules in DCs.

Next, the role of integrin families was investigated in DC adhesion to biomaterials using antibody-blocking techniques to inhibit β_1 and β_2 integrin family members. DC adhesion was measured by assessing the number of non/loosely adherent DCs (an inverse measurement of the number of cells adhering to the substrates) and compared to isotype control treatments. An anti-β_1 blocking antibody (clone P5D2) was unable to affect extent of DC adhesion to both serum-coated (from the culture medium) TCPS or PLGA (Figure 27A) but was able to inhibit DC adhesion and spreading to plasma fibronectin (pFN) coated glass cover slips, demonstrating functionality of the mAb with this ligand pre-coating. Two other monoclonal anti-β_1 blocking antibodies (clones AIIB2 and JB1A) were similarly unable to inhibit DC adhesion to TCPS or PLGA (data not shown). Anti-β_2 pre-treatment using blocking mAb TS1/18, however, at all

concentrations investigated (10, 20 and 40μg/mL) was able to inhibit adhesion of DCs to both TCPS and PLGA films (Figure 27B,C) to levels significantly above isotype controls. The binding ability of anti-β_2 was confirmed via flow cytometry using a fluorescently labeled antibody of the same clone which was unable to bind to DCs when pre-treated with anti-β_2 but successfully bound in the presence of isotype. The morphology of DCs treated with PLGA films was altered from being adherent and spread (Figure 27D) to being rounded (Figure 27E) when β_2 binding was inhibited.

To investigate whether β_2-mediated DC adhesion plays a role in biomaterial-induced DC maturation, CD86 expression was also examined in β_2-blocked DCs cultured on TCPS or treated with PLGA films. On both substrates, a $CD86^{low}$ population was associated with DCs that were pre-treated with anti-β_2, which exemplifies the appearance of immature DCs (Figure 28A). The percentage of DCs in the $CD86^{low}$ gate (shown in Figure 28A, B) was normalized to that of isotype controls for each donor and averaged for quantification. With increasing concentrations of anti-β_2, DCs became more "immature" as the percentage of $CD86^{low}$ DCs increased for DCs cultured on TCPS or treated with PLGA and particularly at 40μg/mL exhibited significantly higher levels of "immature" DCs on both substrates (Figure 28C).

To attempt to identify the α subunit (α_L, α_M and α_X) which pairs with β_2 and determine the complete integrin molecule responsible for DC adhesion and activation by biomaterials, antibody-blocking techniques were also explored. Blocking antibodies against α_L, α_M and α_X were used along with anti-β_2 and the number of non/loosely-adherent DCs were measured as well as the percentage of $CD86^{low}$ DCs for DCs treated with TCPS or PLGA. For DCs cultured on TCPS, antibodies toward α_L, α_M or α_X alone or in combinations with each other were not able to alter extent of DC adhesion (Figure 29A). Once again, blocking β_2 alone (or in combination with α_L or α_X) significantly increased the number of non/loosely-adherent DCs (therefore, decreasing the number of adherent DCs) (Figure 29A). Surprisingly, anti-α_M treatment seemed to lessen the inhibitory capacity of anti-β_2 to prevent adhesion, which was found to possess similar levels of adhesion to that isotype (Figure 29A). As expected, the inhibition of DC adhesion to TCPS by β_2 antibody-blocking matched the reduction in CD86 expression (Figure 29B). Dendritic cells pre-treated with antibodies toward α_L, α_M or α_X showed no shift in the percentage of iDCs ($CD86^{low}$) while DCs pretreated with anti-β_2 (or in combination with α_L or α_X) exhibited a significant increase in the percentage of iDCs (Figure 29B). Also, the anti-α_M pre-treatment, which seemed to prevent anti-β_2 from inhibiting adhesion, similarly appeared to reduce anti-β_2 lowering in CD86 expression by DCs on TCPS to levels found with isotype. For PLGA treatments, similar results were found in that while α subunit antibody-blocking did not affect adhesion (Figure 30A) blocking β_2 alone, or in combination with α_X but not α_L, significantly decreased adhesion and simultaneously lowered CD86 expression (Figure 30A,B). Surprisingly, anti-α_M in combination with either anti-α_L or anti-β_2 showed a slight but significant lowering (compared to isotype) in percentage of $CD86^{low}$ DCs on PLGA which was not found for DCs cultured on TCPS. Overall, while anti-β_2 pre-treatment affected adhesion to a similar degree on both TCPS and PLGA films, it was not as effective in lowering CD86 expression in DCs treated with PLGA as for DC cultured on TCPS (Figures 30B and 30B).

Lastly, to further verify the role of integrins in DC adhesion to biomaterials, both β_1 and β_2 integrin expression and their direct interaction with PLGA films was visualized on PLGA-adherent DCs using confocal microscopy. As shown in Figure 31, DCs expressed low levels of β_1 integrins which did not appear to co-localize with F-actin (Figure 31A) in DC podosomes. In contrast, co-localization of F-actin with β_2 was commonly present in DCs at the sites of adhesion and spreading on PLGA (Figure 31B). Furthermore, cross-linking adherent DCs to the surface of PLGA and removing non-cross-linked cellular components via an SDS solution showed high-levels of β_2 presence at the cross-linked contacts between DCs and PLGA (Figure 31D). The

outlines of DC remnants on PLGA were visible with β_2 visualization but are not observed when examining β_1 (Figure 31C).

Analysis of Transcription Factor Activation Profiles upon DC treatment with pMAs

Although integrins have been recently shown to mediate DC response, the exact mechanisms by which DCs recognize biomaterials remain to be elucidated. In this study, the transcription factor activation profiles of biomaterial-treated DCs were explored for 3h, 6h, and 11h time points. Two pMAs, namely pHEMA and pIBMA, were shown to induce differential TF activation, and their profiles were different from that induced by LPS stimulation. Most notably, pHEMA reduced NF-κB activation by 6h, whereas pIBMA increased NF-κB (Figure 32A), indicating that pIBMA enhanced DC maturation, while pHEMA reduced DC maturation. Furthermore, pHEMA also induced the activation of TFs that have been shown to suppress DC maturation, including E2F-1 and GR/PR (Figure 33A, B) by 6h, whereas pIBMA had no effect on these TFs within the time points examined. pHEMA, but not pIBMA, also induced the activation of NFAT by 11h (Figure 33C), which has been shown to maintain DCs in the immature stage as well as cause apoptotic death of terminally differentiated DCs. Counter intuitively, pHEMA also enhanced the activation of ISRE and HSF (Figure 32B, D), TFs that have been shown to support DC maturation. Interestingly, pHEMA completely eradiated the effect of LPS stimulation on DCs, suggesting that biomaterials can be a powerful immune modulator. The results herein provide a mechanistic insight into biomaterial-induced DC response and can potentially decipher the receptors DCs use to respond to biomaterials.

Role of Serum-Derived Glycans on DC Responses to Biomaterials

The role of carbohydrates in the DC recognition of and response to biomaterials was investigated using several approaches. DCs were cultured in fetal bovine serum (FBS) that had been partially de-glycosylated of carbohydrate ligands using N- and O-glycosidases (Enzymatic CarboRelease Kit ™, QA Bio) with subsequent removal of the cleaved carbohydrate moieties via sequential flows through lectin gel columns (EY labs) using lectins as in ELLAs. However, this resulted in high baseline levels of DC maturation due to endotoxin contamination during this FBS processing making differences in DC maturation on different SAM surfaces indistinguishable and precluding the utility of this approach to assess how the selective absence of carbohydrates in the adsorbed protein layer affected DC maturation. Another deglycosylation approach considered was periodate oxidation of glycoproteins which did reduce the ELLA signal for carbohydrates in the adsorbed protein layers. However, applicability of periodate oxidized biomaterial-adsorbed proteins for DC studies may be confounded by adsorption of serum proteins from the culture media.

An alternative approach which was attempted was to block the carbohydrate moieties of adsorbed proteins, using a optimized in-house synthesized blocking agent comprised of lectin [preliminary studies with *narcissus pseudonarcissus* (NPA) and *ulex europaeus agglutinin II* (UEA-II)] conjugated to bovine serum albumin (BSA), wherein the BSA would provide a “cover” for the carbohydrate moieties to block their interaction with CLRs. However, these optimized lectin-BSA conjugates were not effective in blocking the carbohydrate signal from adsorbed protein using ELLAs. The reasons for this lack of blocking may be due to uncontrollable manner in conjugation of the lectin and BSA which could hinder accessibility of the binding pocket of the lectin for the glycan. Unfortunately, the structure of the lectins does not allow for further specification of the binding site for conjugation and thus no further work is being done to optimize this blocking protocol.

Specific Aim 3: Show that biomaterial chemistry influences the process of DC maturation through an adsorbed protein layer to elucidate the ‘biomaterial associated molecular patterns’ responsible for recognition by immune cells.

SAMs of alkanethiols 1-dodecanethiol, [SH-(CH2)11-CH3], 11-mercapto-undecanol, [HS-(CH2)11OH], 11-mercaptoundecanoic acid, [HS-(CH2)10-COOH] or 11-amino-1-undecanethiol, hydrochloride [C11H26ClNS] (1 mM in absolute ethanol, overnight) with methyl (CH_3), carboxyl (COOH), hydroxyl (OH) or amine (NH_2) functional groups, respectively, were prepared on Ti/Au coated polystyrene or glass flat surfaces according to previously published protocols. A differential profile of carbohydrates was detected using ELLAs in the adsorbed serum protein layer as determined by the underlying biomaterial chemistry of SAMs of alkanethiols presenting different terminal groups[15]. Among SAM endgroups, pre-incubation with 10% serum, as used for DC culture, resulted in differential presentation of CLR ligands; higher α-galactose on COOH SAMs than NH_2 or CH_3 SAMs, highest complex mannose on NH_2 SAMs and higher complex mannose on OH SAMs than CH_3 SAMs[15]. Least sLe^x groups were detected on CH_3 SAMs[15]. Among filtered human serum (HS) eluates from proteins adsorbed to SAM surfaces, complement proteins Factor H, Factor I, coagulation factors antithrombin, prothrombin or proteins such as IgG were present in OH, COOH or NH_2 SAM eluates or in eluates from polystyrene (PS) control surfaces, but not in CH_3 SAM eluates. Among filtered HP eluates, coagulation factor fibrinogen or complement 3 and cell adhesive vitronectin were in PS or all SAM eluates with the exception of CH_3 or COOH respectively and prothrombin was not detected in OH or COOH eluates. Cumulatively, the unique profiles of adsorbed proteins on different SAM chemistries may hence support differential bi-directional interactions with recruited immune/inflammatory cells. Cumulatively, biomaterial chemistry may regulate protein adsorption and hence unique presentation of associated carbohydrates. Differential DC maturation on SAM surfaces was also observed with least mature DCs on CH_3- presenting SAMs, but in the presence of high levels of pro-inflammatory cytokines, with high levels of apoptosis[16].

SDS-PAGE, Western Blotting, 2D Gel Electrophoresis, and Lectin blotting were used to investigate proteins adhered to SAM surfaces of different end groups (-CH_3, OH, COOH, NH_2) on Au/Ti coated polystyrene.

Immunoblot analysis of eluates from SAM surfaces was performed in collaboration with Dr. J.L. Brash and Rena Cornelius at McMaster University[17]. The samples of interest were 1% heat-inactivated filtered human plasma in PBS or 10% heat-inactivated filtered human serum in PBS, similar to protein sources used in DC culture and were prepared and supplied from Georgia Tech. Albumin and apolipoprotein A1 were consistently detected in both filtered h.i 10% HS and 1% HP eluates from all SAM surfaces and from control tissue culture-treated polystyrene (TCPS). Interestingly, Factor H and Factor I, antithrombin, prothrombin, high molecular weight kininogen (HMWK) and IgG were present in eluates from OH, COOH and NH_2 SAM surfaces and in eluates from TCPS, but not in eluates from CH_3 SAM surfaces, following exposure to filtered h.i. 10% HS. These results suggest that CH_3 SAM surfaces were the least pro-inflammatory of all SAM surfaces. Overall, similar trends were observed in the profiles of proteins eluted from surfaces exposed to filtered 10% HS or 1% HP.

Furthermore, in order to elucidate the profiles of carbohydrates present in the eluates from different SAM surfaces as well as the protein sources of these glycosylations, a protocol to perform lectin blotting using NPA, UEA-1, UEA-2, SNA-1 or HHA lectins has been optimized and has been tested on purified single proteins including anti-thrombin III, fibrinogen, albumin, vitronectin, plasminogen known to have these glycosylations. In addition, lectin blotting using NPA, UEA-1, UEA-2, SNA-1 or HHA lectins was performed using plasma or serum samples, following 2D gel electrophoresis. However since several lectins bind the same protein and several proteins bind the same lectin this makes clear trends not distinguishable.

Specific Aim 4: Evaluate the extent of DCs maturation in the presence of biomaterials such that they act as professional APCs in mediating an adaptive immune response to device-associated antigens.

DCs were observed to come in direct contact with PLGA scaffolds, with associated antigen, by immunohistochemical detection. Murine-derived DCs from C57BL/6 mice mature upon contact with PLGA[10]. We showed that ovalbumin (OVA) delivered with PLGA MPs induced a similar level of delayed type hypersensitivity (DTH) response as OVA delivered with the strong adjuvant, CFA[4]. Further, OVA delivered with PLGA MPs induced a higher level of DTH response than PLGA MPs delivered without OVA.

The biomaterial adjuvant effect of PLGA in the form of MPs (6 μm) or porous scaffolds in supporting a humoral immune response towards adsorbed model antigen, ovalbumin (OVA) was demonstrated. Ovalbumin adsorbed and co-delivered with biomaterial carrier vehicles supported a moderate OVA-specific humoral immune response that was maintained for the 18 wk duration of the experiment[18]. This humoral immune response was primarily Th2 helper T cell-dependent as indicated by the predominant IgG1 isotype. Furthermore, the *in vivo* proliferation [reduction in 6-carboxyfluorescein diacetate succinimidyl ester (6-CFSE) fluorescence] of fluorescently-labeled adoptively transferred OVA-specific $CD4^+$ T cells from transgenic OT-II mice in the presence of OVA adsorbed and co-delivered with a biomaterial was similar to that observed for antigen delivered with CFA (Figure 34)[19]. Thus, we have shown that the biomaterial acted as an adjuvant in the development of an adaptive immune response to co-delivered antigen.

To correlate the *in vitro* differential effects of biomaterials on DC maturation with the resultant adjuvant effect *in vivo*, we hypothesized that PLGA SCs would support a stronger murine adaptive immune response to controlled released co-delivered antigen than agarose SCs. At 12 wks, mice receiving porous PLGA SCs delivering OVA (similar to mice receiving OVA with the strong adjuvant, CFA, the positive control) were found to have significantly higher anti-OVA antibody concentrations than mice receiving OVA with PBS (negative control) (Figure 34)[20]. In contrast, mice receiving porous agarose SCs delivering OVA were not shown to be significantly different the anti-OVA antibody concentrations from mice receiving OVA with PBS. Serum concentrations of IgG and IgG1 from mice receiving treatments with OVA had similar profiles, while IgG2a production was detected only for CFA treatment with OVA. Mice receiving either SC without incorporated OVA did not have detectable levels of anti-OVA antibody production. Therefore, porous PLGA SCs were shown to induce a biomaterial adjuvant effect to enhance specific antibody production, which was not observed with porous agarose SCs. Hence, biomaterial selection as SCs can differentially affect the adaptive immune response to a co-delivered antigen. Furthermore, we have validated the *in vitro* assessment of biomaterial effects on DC maturation in predicting the *in vivo* biomaterial adjuvant effect to co-delivered antigen.

We have evidence of biomaterial-implant site associated 'danger signals' or DAMPs. To assess the differential level of enhancement of the immune response depending on the form of carrier vehicle (MPs vs. scaffold) and the extent of tissue injury due to its delivery, the total amounts of polymer and OVA delivered were kept constant as well as the release rate of OVA for both carrier vehicles. The level of the humoral immune response was higher and sustained for OVA released from PLGA SCs which were implanted with associated tissue damage, and lower and transient when the same amount of polymer and OVA were delivered from PLGA MPs, which were minimally invasively delivered by injection[21]. These results implicate 'danger signals' or DAMPs associated with the implantation of the scaffolds due to tissue injury which primed the system for an enhanced immune response and a biomaterial adjuvant effect. These results indicate that it is important to deliver/implant a tissue engineered construct as non-invasively as possible to minimize any potential immune responses. Furthermore, there is the

potential to 'hide' an immunological tissue engineered construct if it is delivered in such a manner as to avoid 'danger signals'.

To identify biomaterial-implant site associated 'danger signals', exudates were prepared of the tissue surrounding dorsally, subcutaneously, implanted PLGA SCs with adsorbed OVA or without OVA after one week of implantation in C57BL/6 mice. Alternatively, some animals were used as naïve controls. Biomaterial/tissue exudates were analyzed by sodium dodecyl sulphate-polyacrylamide gel electrophoresis (SDS-PAGE) gels and immunoblotting for heparin/heparan sulfate, HSP70, HSP60, HSP90, HMGB1, interferon-α, fibronectin and fibrinogen. By immunoblot analysis, all probed-for 'danger signals' were detected in the naïve control sample or exudates prepared from PLGA or PLGA/OVA scaffold implants, however, to different extents[22]. Of particular note, was the fact that higher levels of HMGB1 were detected in PLGA or PLGA/OVA samples, as compared to the naive controls. Moreover, high levels of fibrinogen and fibronectin were detected in the naive controls as compared to PLGA or PLGA/OVA samples. Therefore, HMGB1 may be released at the implant site by necrotic cells or by inflammatory cells, resulting in its higher detection in tissue exudates than the naïve controls. Similarly, it would have been expected that HSPs would also have been detected in the biomaterial exudates to a greater extent than in the naïve controls. The lower levels of fibrinogen and fibronectin associated with biomaterial exudates may be due to the local adsorption of these proteins to the biomaterial surface sequestering them from the surrounding tissue.

Publications:

Cornelius, R.M., Shankar, S.P., Brash, J.L., **Babensee, J.E.,** Immunoblot Analysis Of proteins Associated With Self-Assembled Monolayer Surfaces Of Defined Chemistries. J. Biomed. Mater. Res., in press.

Kou, P.M., Schwartz, Z., Boyan, B.D., **Babensee, J.E.,** Dendritic cell responses to surface properties of clinical titanium implants, Acta Biomaterialia, 7:1354-1363 (2011).

Kou PM, **Babensee JE,** Relevance of Macrophage and Dendritic Cell Phenotypic Diversity in the Context of Biomaterials, J. Biomed. Mater. Res., 96A:239–260 (2011).

Rogers, T., **Babensee, J.E.,** The Role of Integrins in the Recognition of Biomaterials by Dendritic Cells, Biomaterials, 32:1270-1279 (2011).

Norton, L., Park, J., **Babensee, J.E.,** Biomaterial adjuvant effect is attenuated by material selection or anti-inflammatory delivery, Journal of Controlled Release, 146:341-348 (2010).

Kou, P.M., **Babensee, J.E.**, Validation of a High Throughput Methodology to Assess the Effects of Biomaterials on Dendritic Cell Phenotype, Acta Biomaterialia, 6:2621-2630 (2010).

Rogers, T.H., **Babensee, J.E.**, Altered Adherent Leukocyte Profile on Biomaterials in Toll-like Receptor 4 Deficient Mice, Biomaterials, 31:594–601 (2010).

Shankar, S.P., Petrie, T.A., García, A.J., **Babensee, J.E.,** Dendritic Cell Responses To Self-Assembled Monolayers Of Defined Chemistries**,** J. Biomed. Mater. Res., 92A: 1487–1499 (2010).

Shankar, S.P., Chen, I.I., Keselowsky, B.G., García, A.J., **Babensee, J.E.,** Profiles Of Carbohydrate Ligands Associated With Adsorbed Proteins On Self-Assembled Monolayers Of Defined Chemistries, J. Biomed. Mater. Res., 92A: 1329–1342 (2010).

Shankar, S.P., and **Babensee, J.E.,** Comparative Characterization Of Cultures Of Primary Human Macrophages Or Dendritic Cells For Biomaterial Studies, J. Biomed. Mater. Res. 92A: 791–800 (2010).

Babensee, J.E,. Interaction of Dendritic Cells with Biomaterials, Seminars in Immunology 20: 101–108 (2008)

Yoshida M, Mata J, **Babensee JE.** Effect of poly(lactic-*co*-glycolic acid) contact on maturation of murine bone-marrow derived dendritic cells. J. Biomed. Mater. Res., 80A: 7-12, (2007).

Yoshida M, **Babensee, JE.** Differential effects of agarose and poly(lactic-*co*-glycolic acid) on dendritic cell maturation. J. Biomed. Mater. Res., 79A: 393-408 (2006).

Yoshida M, **Babensee JE.** Molecular aspects of microparticle phagocytosis by dendritic cells. Journal of Biomaterial Science, Polymer Edition, 17: 893-907 (2006).

Babensee JE, Paranjpe A. Differential levels of dendritic cell maturation on biomaterials used in combination products. J. Biomed. Mater Res., 74A:503-510 (2005).

Publications In Preparation:

Park, J., **Babensee, J.E**., Differential Functional Effects Of Biomaterials On Dendritic Cell Maturation, J. Biomed. Mater. Res., to be submitted.

Park, J., **Babensee, J.E.**, *In Vitro* Control Of Dendritic Cell Phenotype By Scaffolds For Tissue Engineering, J. Biomed. Mater. Res., to be submitted.

Park, J., Gerber, M.H., **Babensee, J.E.**, Phenotype And Polarization Of Autologous T Cells By Biomaterial-Treated Dendritic Cells, Biomaterials, to be submitted.

Rogers, T., **Babensee, J.E.,** Characterization of adherent and non/loosely adherent murine bone marrow derived dendritic cells and their responsiveness to maturation stimuli, J. Immunological Methods, under 1st revision.

Kou PM, Patel R, Cunningham B, Pallassana N, Kohn J, **Babensee JE.** Polymethacrylates mediated differential dendritic cell phenotype through distinct transcription factor activation profiles. Biomaterials, in preparation.

Kou PM, Browning R, Joy A, Cunningham B, Kohn J, and **Babensee JE.** Predicting dendritic cell phenotype from surface properties in a terpolymer library using multivariate analysis. Integrative Biology, in preparation.

Kou PM, Joy A, Pallassana N, Cunningham B, Kohn J, **Babensee JE.** Biomaterial property-dendritic cell (DC) phenotype relationships elucidated through multivate analysis of DC responses to a polymethacrylate combinatorial library. Biomaterials, in preparation.

References

[1] Shankar SP, Babensee JE. Comparative Characterization Of Cultures Of Primary Human Macrophages Or Dendritic Cells For Biomaterial Studies. J Biomed Mater Res, submitted.
[2] Babensee JE, Paranjpe A. Differential levels of dendritic cell maturation on biomaterials used in combination products. J Biomed Mater Res 2005;74A:503-510.
[3] Yoshida M, Babensee JE. Differential effects of agarose and poly(lactic-co-glycolic acid) on dendritic cell maturation. J Biomed Mater Res 2006;79A:393-408.
[4] Yoshida M, Babensee JE. Poly(lactic-co-glycolic acid) enhances maturation of human monocyte-derived dendritic cells. J Biomed Mater Res 2004;71A:45-51.
[5] Yoshida M, Babensee JE. Molecular aspects of microparticle phagocytosis by dendritic cells. J Biomat Sci. Polym Ed 2006;17:893-907.
[6] Kou PM, Babensee JE. Validation of a High Throughput Methodology to Assess the Effects of Biomaterials on Dendritic Cell Phenotype. Acta Biomaterialia 2010;6:2621-2630.
[7] Ishaug SL, Crane GM, Miller MJ, Yasko AW, Yaszemski MJ, Mikos AG. Ectopic bone formation by marrow stromal osteoblast transplantation using poly(DL-lactic-co-glycolic acid) foams implanted into the rate mesentery. J Biomed Mater Res 1997;36:17-28.
[8] Lee J, Shanbhag, S, Kotov NA. Inverted colloidal crystals as three-dimensional microenvironments for cellular co-cultures. J Mater Chem 2006;16:3558-3564.
[9] Kou PM, Schwartz Z, Boyan BD, Babensee JE. Dendritic cell responses to surface properties of clinical titanium implants. Acta Biomaterialia, 2011;7:1354-1363.
[10] Yoshida M, Mata J, Babensee JE. Effect of poly(lactic-co-glycolic acid) contact on maturation of murine bone-marrow derived dendritic cells. J. Biomed. Mater. Res., 2007, 80A, 7-12.
[11] Poltorak A, He X, Smirnova I, Liu M, Huffel C, Du X, et al. Defective LPS signaling in C3H/HeJ and C57BL/10ScCr mice: mutations in Tlr4 gene. Science 1998;282:2085-2088.
[12] Rogers TH, Babensee JE. Altered Adherent Leukocyte Profile on Biomaterials in Toll-like Receptor 4 Deficient Mice. Biomaterials. 2010;31:594–601.
[13] Xiaowei W. and Seed B. A PCR primer bank for quantitative gene expression analysis. Nucleic Acids Research 2003;31:e154;1-8.
[14] Rogers T, Babensee JE, The Role of Integrins in the Recognition of Biomaterials by Dendritic Cells, Biomaterials, 2011;32:1270-1279.
[15] Shankar SP, Chen II, Keselowsky BG, García AJ, Babensee JE. Profiles Of Carbohydrate Ligands Associated With Adsorbed Proteins On Self-Assembled Monolayers Of Defined Chemistries. J Biomed Mater Res 2010;92A:1329–1342.
[16] Shankar SP, Petrie TA, García AJ, Babensee JE. Dendritic Cell Responses To Self-Assembled Monolayers Of Defined Chemistries. J Biomed Mater Res 2010;92A:1487–1499.
[17] Cornelius RM, Shankar SP, Brash JL, Babensee JE. Immunoblot Analysis Of proteins Associated With Self-Assembled Monolayer Surfaces Of Defined Chemistries. J Biomed Mater Res, in press.
[18] Matzelle MM, Babensee JE, Humoral immune responses to model antigen delivered with biomaterials used in tissue engineering. Biomaterials 2004;25:295-304.
[19] Babensee JE, Stein MM, Moore L. Interconnections Between Inflammatory and Immune Responses in Tissue Engineering. Ann NY Acad Sci. 2002;961:360-363.
[20] Norton L, Park J, Babensee JE. Biomaterial adjuvant effect is attenuated by material selection or anti-inflammatory delivery. J Controlled Rel. 2010;146:341-348.
[21] Bennewitz N, Babensee JE. The effect of the physical form of poly(lactic-co-glycolic acid) carriers on the humoral immune response to co-delivered antigen. Biomaterials 2005;26:2991-2999.
[22] Babensee JE. Interaction of Dendritic Cells with Biomaterials. Seminars in Immunology 2008;20:101–108.

Final Progress Report
April 1, 2011.
NIH 1RO1EB004633-01A1
Dendritic Cell Phenotype Upon Contact With Biomaterials
P.I.: Julia E. Babensee

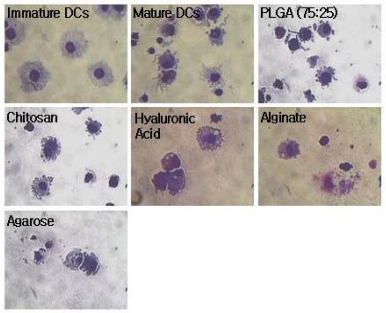

Figure 1: Dendritic cells cultured on different polymer films show variation in cell morphology. (Original Mag: 40 ×)

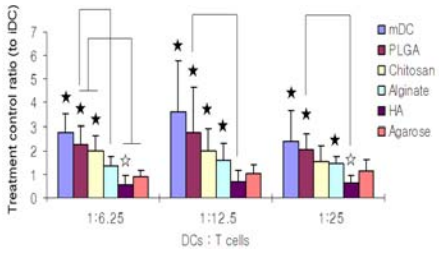

Figure 2: Allostimulatory capacities in MLR for DCs cultured on biomaterial films. Ratios to the immature DCs; mean±SD, n=6 independent donors. ★: $p \le 0.05$, higher than iDC; ☆: $p \le 0.05$, lower than I DC; Brackets: $p \le 0.05$, statistically different between two biomaterial treatments; '⊥' indicates 'or'.

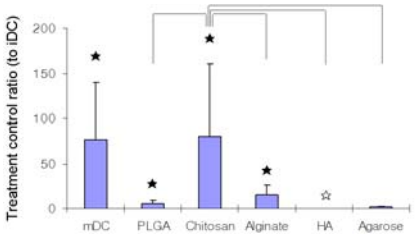

Figure 3: Differential levels of TNF–α release (normalized to DNA amounts) upon DC treatment with biomaterial films. Ratios to iDCs; mean±SD, n=6 independent donors. ★: $p \le 0.05$, higher than iDC; ☆: $p \le 0.05$, lower than iDC; Brackets: $p \le 0.05$, statistically different between two biomaterial treatments.

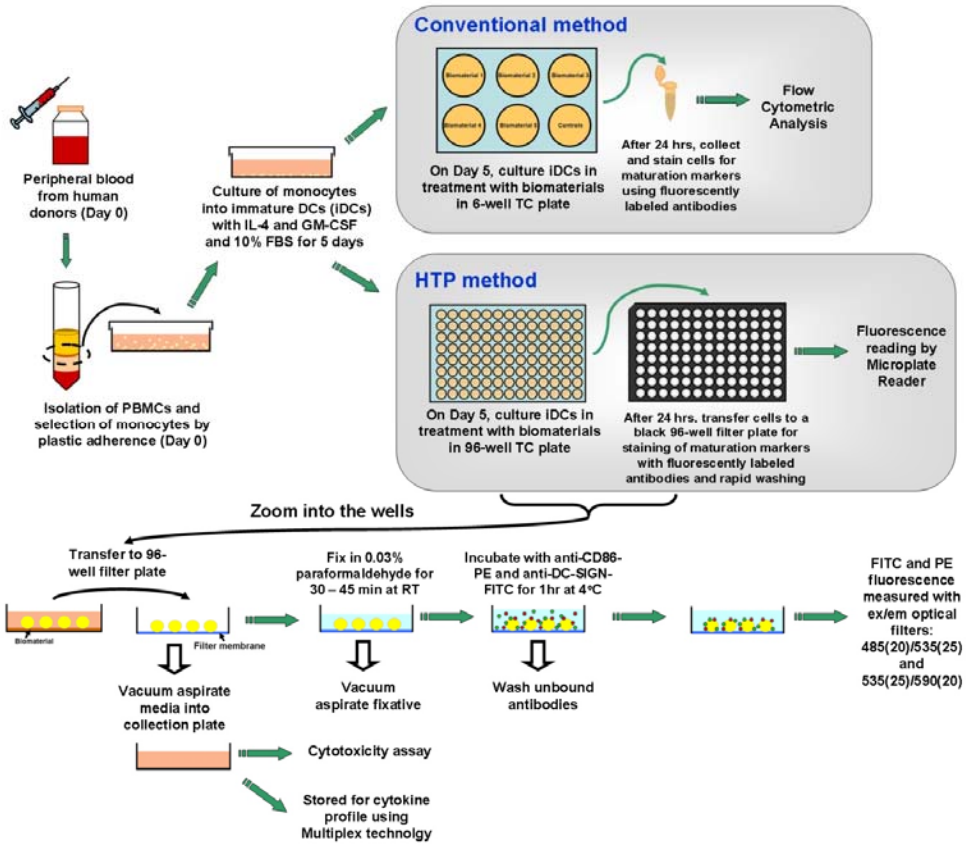

Figure 4: A schematic of the conventional method and the HTP method for studying DC response to biomaterials. For both of the methods, DCs are derived from human peripheral blood monocytes using the same procedures until day 5. On day 5, for the conventional method, DCs are cultured on biomaterials inserted in a 6-well plate for 24 hours. The cells after treatment are then collected and stained, and flow cytometry is performed to analyze the cell surface marker expression. In contrast, for the HTP method, DCs are cultured on 96-well plates coated with different biomaterials for 24 hours. On day 6, DCs are transferred to a 96-well filtration plate, fixed and subsequently stained with anti-CD86-PE and anti-DC-SIGN-FITC antibodies for 1 hour and washed. The relative fluorescence intensity is subsequently measured by a Tecan Infinite F500 microplate reader. Simultaneously, the cell culture supernatants from each well can be aspirated into a collection plate for immediate cytotoxicity assessment or stored for cytokine profiling experiment

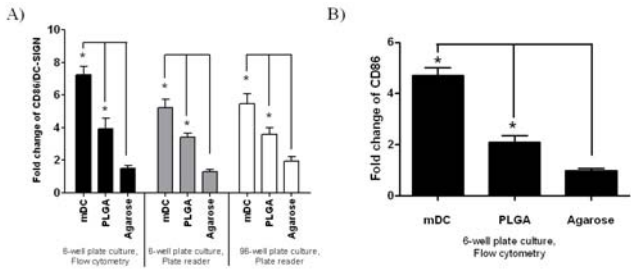

Figure 5: Biomaterial study with PLGA and agarose. A) Fold changes of maturation factor (defined as CD86/DC-SIGN) are shown with mean ± SEM; n=8 (6 donors). Comparison of fold change of CD86/DC-SIGN expression for DCs treated with biomaterials in the 6-well format by FC (black bars), 6-well format by fluorescent plate read (grey bars), and 96-well format by fluorescent plate read (white bars), as compared to iDCs. B) Fold change of CD86, the conventional analysis of DC maturation by flow cytometry, are shown with mean ± SEM, n=8 (6 donors). For statistical comparison of mDCs and biomaterial treatments in pairs, the general linear model of ANOVA pairwise with mixed model was used. *: $p<0.05$, statistically different from iDCs and higher than iDCs. Brackets: $p<0.05$, statistically different between two biomaterial treatments or between biomaterial treatment and mDCs.

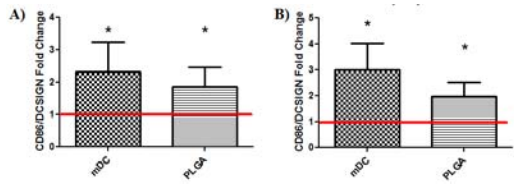

Figure 6: : DC response to polymer (PLGA) as compared to LPS (mDC) in a 384 well plate (B) as compared to in a 96 well plate (A). No statistical difference can be seen between the two different assay formats. Data normalized to iDC on TCPS for fold change and presented as mean±S.D.; n = 6 independent donors; * = Statistical difference from cultured iDCs on TCPS, $p \leq 0.05$.

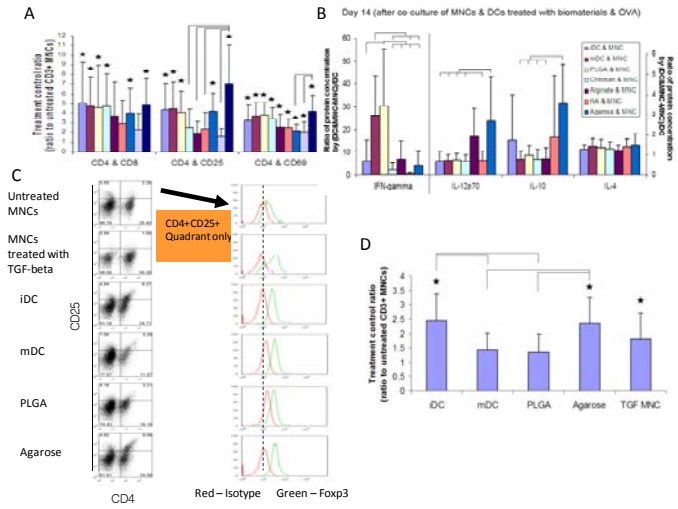

Figure 7: A) Percentage numbers in double positive quadrant dot plots of CD4 & CD8, CD4 & CD25, CD4 & CD69 expression on autologous CD3+ T cells upon co-culture with DCs treated with different biomaterial films and OVA antigen. Ratios to the untreated CD3+ MNCs are shown with mean±SD, n=6 donors (6 independent experiments with different donors). ★$p \leq 0.05$, compared to control and higher than control; ☆$p \leq 0.05$, compared to control and lower than control; Brackets: $p \leq 0.05$, statistically different between two T cells for DCs treated with different biomaterial films. B) Geometric mean fluorescence intensity (gMFI) of cytometric bead array (CBA) for interferon (IFN)-gamma, IL-12p70, IL-10, IL-4 release for DCs treated with different biomaterial films or with OVA antigen. Cytokines were measured using the supernatant saved on Day 6 (after 24 hour-treatment of DCs with biomaterial films with or without antigen). Ratios to the immature DCs are shown with mean±SD, n=6 donors (6 independent experiments with different donors). ★$p \leq 0.05$, compared to immature DCs and higher than immature DC; ☆$p \leq 0.05$, compared to immature DCs and lower than immature DC; Brackets: $p \leq 0.05$, statistically different between two T cells for DCs treated with different biomaterial films. C) Foxp3 expressions on autologous CD3+ T cells upon co-culture with DCs treated with different biomaterial films (PLGA or agarose) and OVA antigen. Representative plots for one donor were selected from all 6 donors. Y-axis for all plots indicates CD25 expression while X-axis for all plots indicates CD4 expression. Numbers shown in each quadrant indicate the percentage of events for each quadrant. Representative histograms (from all 6 donors) for Foxp3 expressions on CD4+CD25+ T cells gated from the quadrant dot plots. gMFI of Foxp3 expressions on gated CD4+CD25+ T cells. TGF MNC indicates MNCs treated with TGF-β to induce Foxp3+ from CD4+ T cells. gMFIs of the isotype were subtracted from gMFIs of FoxP3 per control or treatment and then, ratios to the untreated CD3+ MNCs are shown with mean±SD, n=6 donors (6 independent experiments with different donors). ★$p \leq 0.05$, statistically higher than control (=1); ☆$p \leq 0.05$, statistically lower than control (=1); Bracket: $p \leq 0.05$, statistically different between two T cells for DC treatments with different biomaterial films.

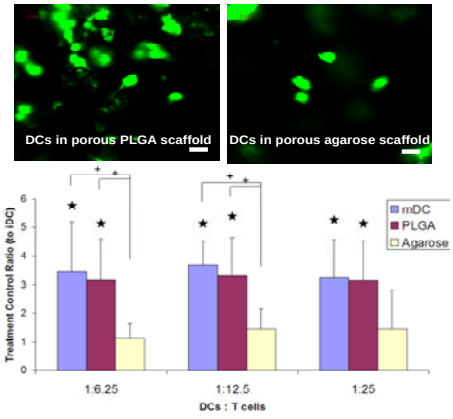

Figure 8: Morphology of calcein-labeled DCs seeded in porous PLGA or agarose scaffolds. Allostimulatory capacity of DCs treated with porous PLGA or agarose scaffolds in MLRs. Ratios to iDCs; mean±SD, n=6 independent donors. ★: $p \leq 0.05$, higher than iDC; ☆: $p \leq 0.05$, lower than iDC; Brackets: $p \leq 0.05$, statistically different between two biomaterial treatments.

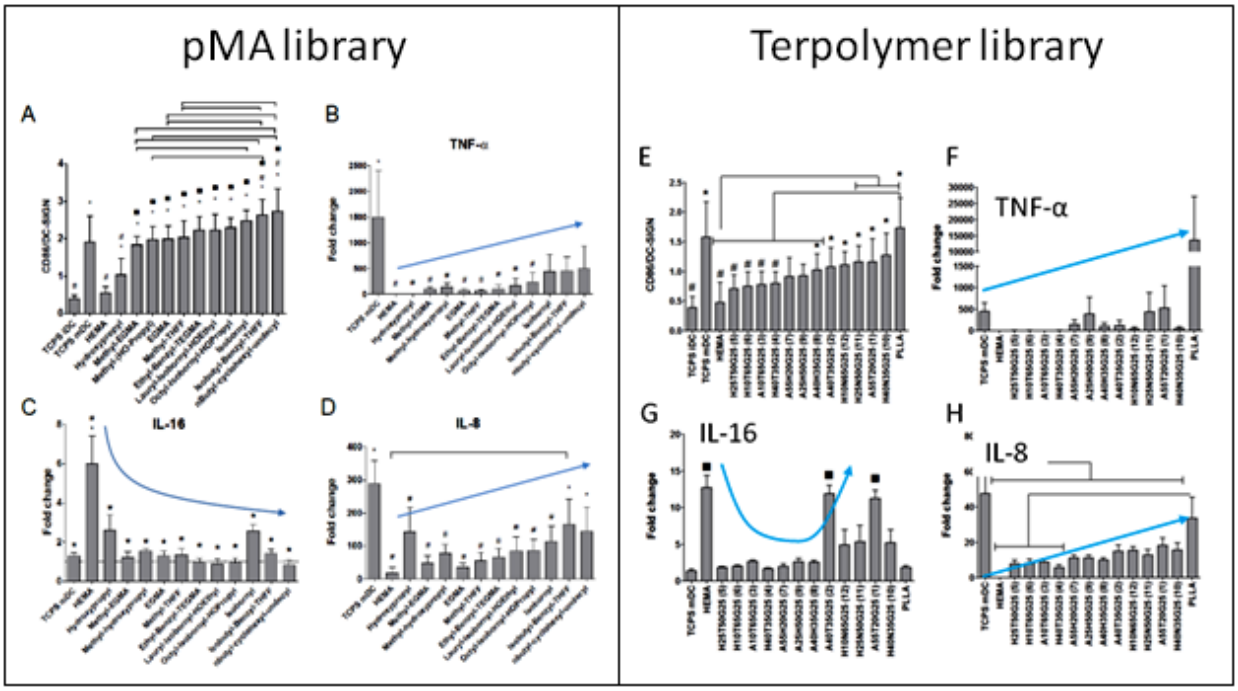

Figure 9: DC phenotype in response to treatment with different pMAs (A – D) or terpolymers (E – H). A,E: The DC maturation metric, CD86/DC-SIGN, is shown as mean±SEM with n = 11 experiments (6 different donors) for pMAs and n=6 for terpolymers. B,F: TNF-α production. C,G: IL-16 production. D,H: IL-8 release; cytokine productions normalized to those of immature DCs (iDCs).

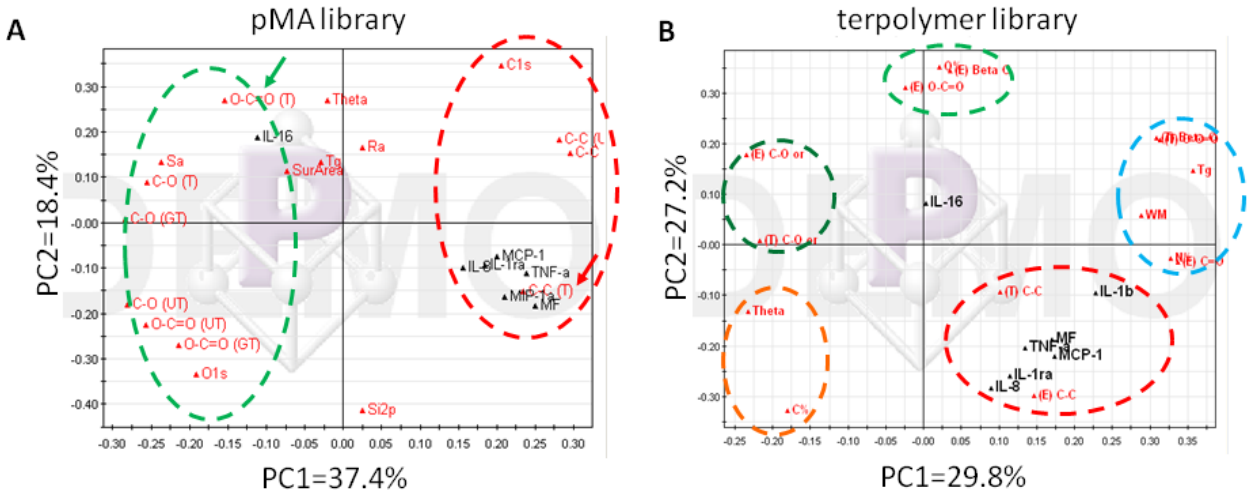

Figure 10: Assessment of material property–DC phenotype relationships using PCA loadings plot for pMA (A) or terpolymer library (B). For pMA library (A), PC1 represents 37.4% of data variance, and PC2 explains 18.4% of data variance (total = 55.8%). Surface carbon (red dotted ellipse) is associated with DC maturation. In particular, theoretical C-C [C-C (T)] bond clusters with the phenotype variables (red arrow), suggesting its strong correlation with DC maturation. In contrast, surface oxygen locates on the opposite end of the PC1 and far away from the maturation phenotype, suggesting its associated with an iDC phenotype. In particular, theoretical O-C=O bond [O-C=O (T)] clusters the most closely with IL-16, which is an anti-inflammatory cytokine in this situation. Ra (line roughness), Tg, surface area, and contact angle are not determinant of the overall DC phenotype, but they contribute to some extent to the production of IL-16, as seen by their similar positioning along PC2. Note: There are three types of chemical composition values: T, UT, and GT. T=theoretical; UT=experimental at U of Toronto; GT=experimental at Georgia Tech. For terpolymer library (B), PC1 represents 29.8% of data variance, and PC2 explains 27.2% of data variance (total = 57%). Similar to pMA library, surface carbon (red dotted ellipse) is strongly correlated with DC maturation. Material properties such as Tg, WM, % nitrogen, and C=O group appeared to be associated with DC maturation along PC1 (blue dotted ellipse), while contact angle (Theta) and % carbon are associated with DC maturation along PC2 (orange dotted ellipse). In contrast, single-bond C-O, whether experimental (E) or theoretical (T), is negatively correlated with DC maturation by locating at the diagonally opposite quadrant of the DC phenotype variables (dark green ellipse). In addition, carboxyl groups (light green ellipse) do not contribute to PC1, but are situated away from DC maturation phenotype along PC2, suggesting that these material properties are also associated with an iDC phenotype.

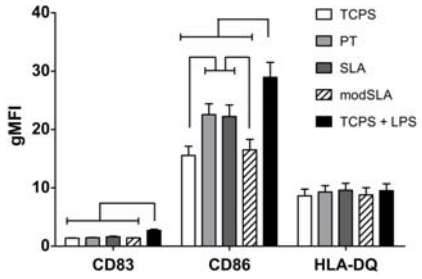

Figure 11: Dendritic cell phenotype in response to Ti surfaces with different roughness and chemistry. The raw geometric mean fluorescence intensities (gMFI) are shown as mean±SEM with n = 12 different donors. *: p<0.05 different from TCPS-treated iDCs; #: p<0.05 different from TCPS + LPS-treated mDCs; Brackets: p<0.05 different among treatments. The immature DCs are treated with TCPS, PT, SLA, modSLA, or TCPS + LPS, respectively. TCPS-treated iDCs would be the negative control of immature DCs, while the TCPS- and LPS-treated iDCs became the positive control of mature DCs. TCPS: tissue-culture polystyrene; PT: pre-treated Ti; SLA: acid etched and grit blasted Ti; modSLA: hydrophilic SLA.

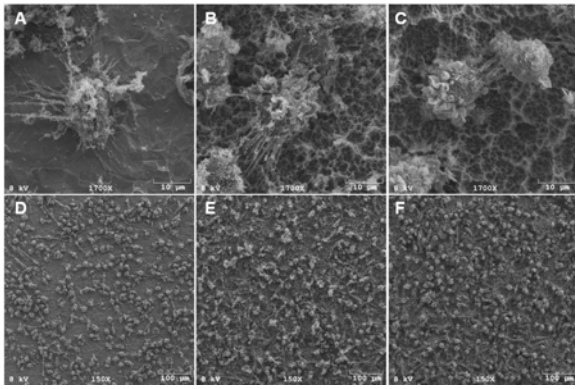

Figure 12: SEM of DCs on Ti surfaces. High magnification micrographs (1700x) show that DCs on PT (A, D) or SLA (B, E) exhibited highly dendritic morphology, which is associated with mDCs; DCs on modSLA (C, F) exhibited rounded morphology, which is associated with iDCs. Low magnification scans (150x) (D, E and F) show that the different Ti surfaces adhere similar numbers of DCs. Data are from one of two separate experiments, both with comparable results.

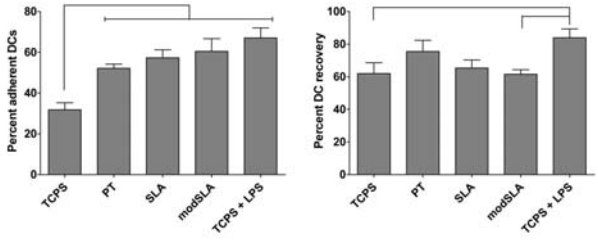

Figure 13: Percent adherent cells on and percent DC recovery from the Ti substrates and controls. Left: Percent of cells (adherent DCs/recovered DCs) adherent to the different Ti surfaces (PT, SLA or modSLA) was not significantly different from each other. Right: Percent DC recovery from modSLA was lower compared to mDC control (TCPS+LPS). n=6 donors (mean±SEM). Brackets represent statistical significance among treatments with p≤0.05.

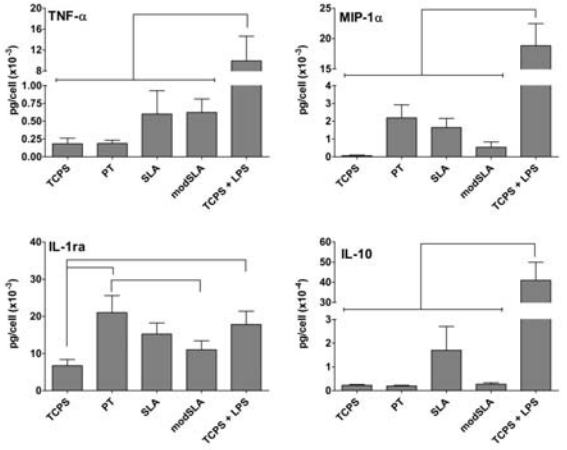

Figure 14: Cytokine and chemokine release for DCs treated with Ti surfaces (PT, SLA or modSLA) as compared to the iDC (TCPS) and mDC (TCPS+LPS) controls. The cytokine amount was normalized to the total cell number in the well. n=12 donors (mean±SEM). Brackets represent statistical significance among treatments with p≤0.05.

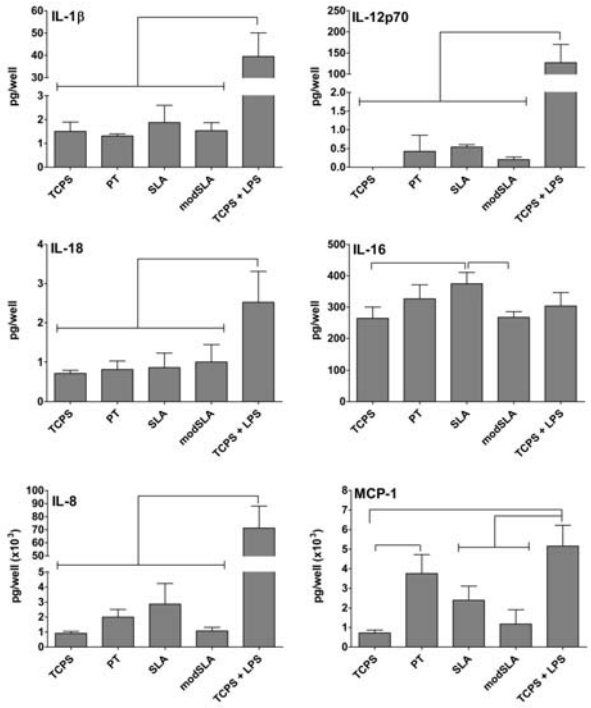

Figure 15: Cytokine and chemokine release for DCs treated with Ti surfaces (PT, SLA or modSLA) as compared to the iDC (TCPS) and mDC (TCPS+LPS) controls. The cytokine amount produced by the cells in the well is shown. n=3 donors (mean±SEM). Brackets represent statistical significance among treatments with p≤0.05.

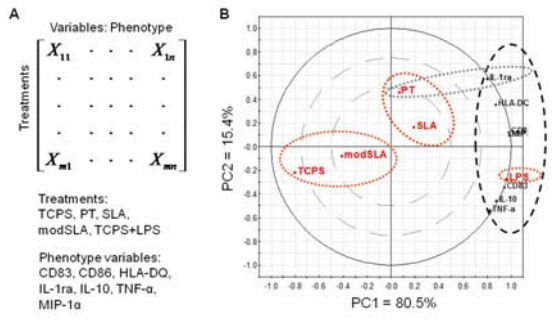

Figure 16: Confirmation of the relative effects of Ti substrates (PT, SLA or modSLA) on DC phenotype relative to the iDC (TCPS) and mDC (TCPS+LPS) controls using PCA. (A) The organization of data into a matrix for PCA. (B) PCA biplot of the DC phenotype variables, including surface marker expression of CD83, CD86 and HLA-DQ and production of TNF-α, IL-1ra, IL-10 and MIP-1α, for PT, SLA, modSLA, TCPS and LPS treatments of DCs. PC1 represents 80.5% of data variance, and PC2 explains 15.4% of data variance, which together capture 95.9% of data variance with little loss of information. The red dotted ellipses represent clustering of similar treatment groups (e.g. TCPS and modSLA form one cluster, while PT and SLA form another cluster). The thick black dotted ellipse indicates the location of phenotype variables, which is strongly associated with LPS-treated DCs along the far end of PC1. The gray dotted ellipse represents the association of PT treatment and IL-1ra release along PC2.

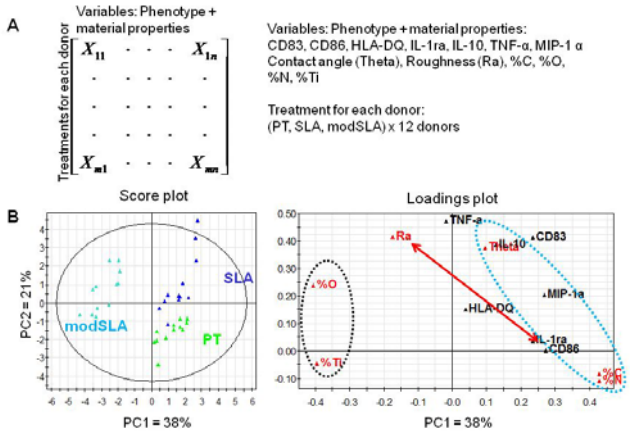

Figure 17: Assessment of Ti material property–DC phenotype relationships using PCA. (A) The organization of the data into a matrix for PCA. (B) PCA score plot and loadings plot for the first two PCs. PC1 represents 38% of data variance, and PC2 explains 21% of data variance, which together capture 59% of data variance. The red double-headed vector indicates that CD86 and Ra primarily influence PC1 and PC2, respectively, suggesting that roughness has little effect on CD86 expression. The blue dotted ellipse indicates that material properties of air-water contact angle (Theta), surface %C and %N are more associated with the phenotype variables. Conversely, the black dotted ellipse shows that properties such as %O and %Ti are situated on the opposite side of the phenotype variables, suggesting that these material properties are more associated with an iDC phenotype. The data set can be best modeled by 3 PCs that capture a total of 74.4% information. However, because score plot and loading plots of PC1 and PC3 yield similar conclusions as those of PC1 and PC2, and because plots of PC2 and PC3 do not yield meaningful information, only the plots of PC1 and PC2 are shown for simplicity.

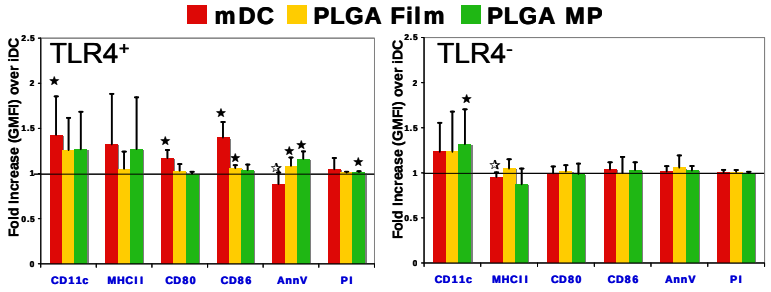

Figure 18: FC gMFIs for treated murine DCs derived from C57BL/10ScSnJ (TLR4^{+}) or C57BL/10ScNJ (TLR4^{-}) normalized to iDC; mean±SD; n=6 mice. ★p < 0.05, greater than iDC; ☆: p < 0.05, less than iDC,.

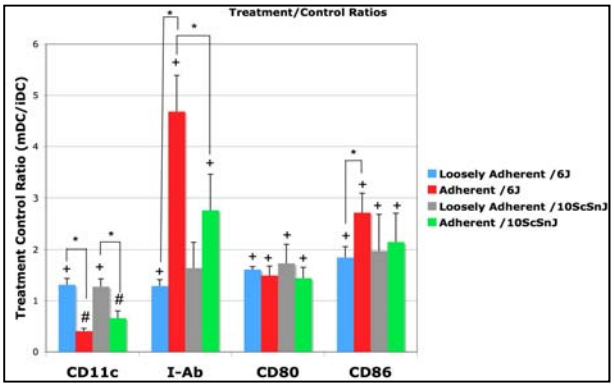

Figure 19: Response of adherent and loosely-adherent BMDCs from C57BL/6J or C57BL/10ScSnJ to ultrapure-LPS. Mean±S.D.; n=3 +: $p < 0.05$, greater than iDC; #: $p < 0.05$, less than iDC; *: $p < 0.5$ difference between loosely and loosely-adherent.

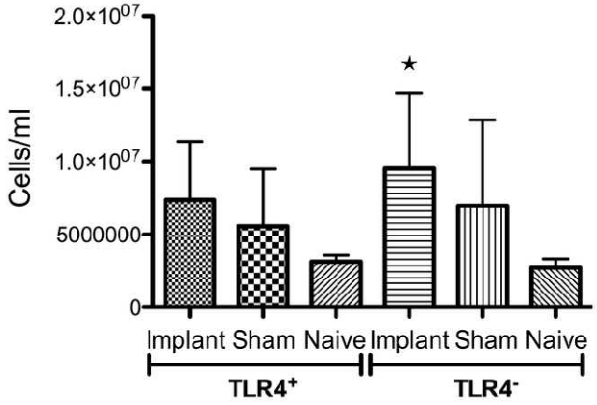

Figure 20: Total leukocyte concentrations in IP lavages for $TLR4^+$ or $TLR4^-$ mice receiving a PET disc implant, sham surgery or in the naïve control group.★; $p<0.05$ in comparison to either naïve group, n=7-9 mice per group. Bars represent mean+SD.

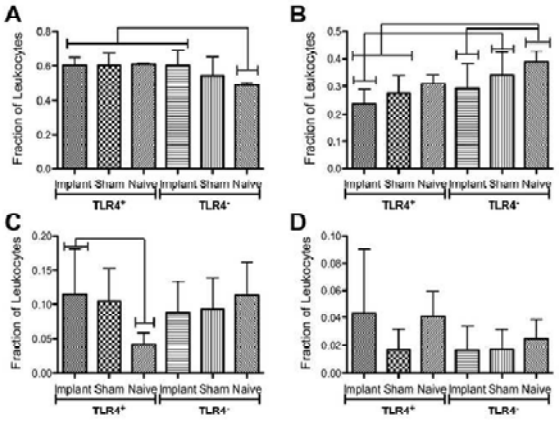

Figure 21: Differential leukocyte profiles showing fractions of (A) Neutrophils, (B) Monocyte/Macrophages, (C) Eosinophils, (D) Lymphocytes in IP lavages for $TLR4^+$ or $TLR4^-$ mice receiving a PET disc implant, sham surgery or naïve control. Brackets indicate significant differences between groups ($p<0.05$), n=7-9 mice per group. Bars represent mean+SD.

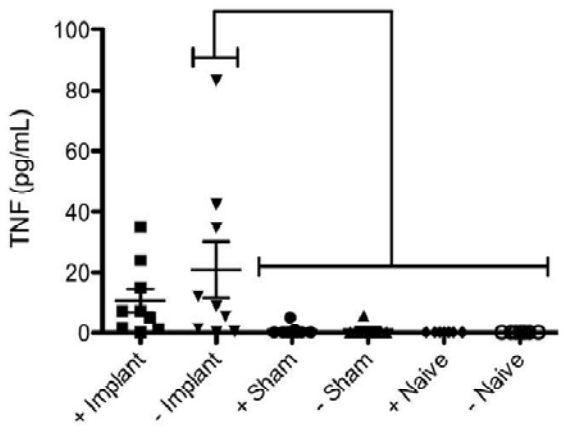

Figure 22: TNF-α concentrations in IP lavages for $TLR4^+$ (+) or $TLR4^-$ (-) mice receiving a PET disc implant (Implant), sham surgery (Sham) or naïve control (Naïve). Individual mouse concentrations are plotted as points with horizontal lines representing mean with standard deviations. Brackets indicate statistical difference ($p<0.05$) between group, n=7-9 mice per group.

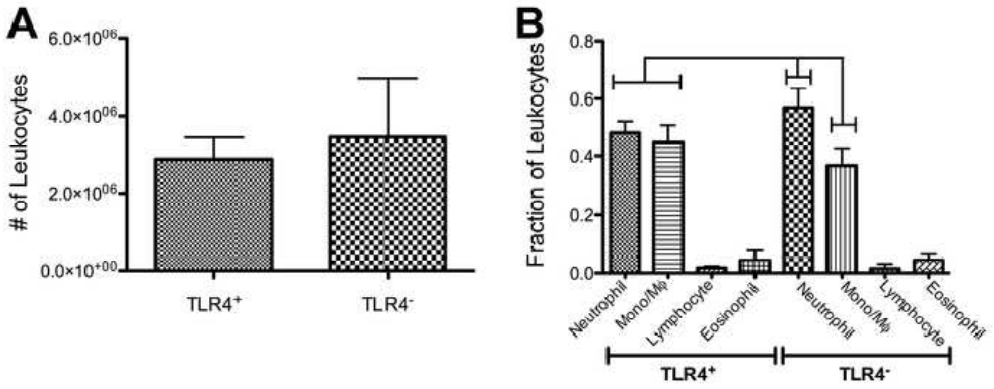

Figure 23: Adherent leukocyte profiles on PET discs following 16hr of IP implantation into $TLR4^+$ or $TLR4^-$ mice. (A) Total number of adherent leukocytes collected from implants in either strain. No statistical difference was found between strains ($p=0.27$); n=7-9 mice per group. (B) Adherent leukocyte profiles showing fractions of neutrophils, monocyte/macrophages, eosinophils, and lymphocytes. Brackets indicate significant differences between groups ($p<0.05$); n=7-9 mice per group. All treatments significantly different from each other except for lymphocyte and eosinophil fractions from either strain as well as neutrophil and monocyte/macrophage fractions from $TLR4^+$ strain.

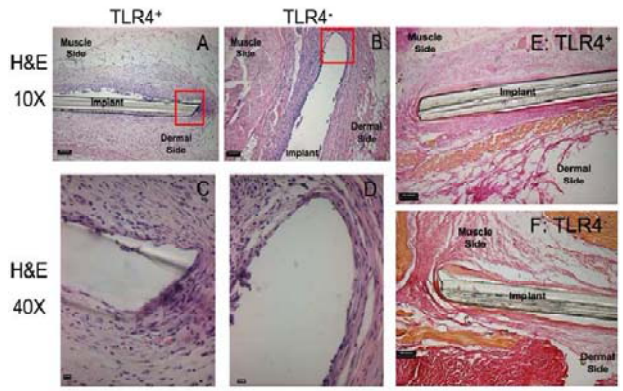

Figure 24: Representative H&E and Van Gieson stained tissue sections of PET discs implanted SC for 2 weeks. Shown are 10X images of representative H&E stained sections from a $TLR4^+$ (A) or a $TLR4^-$ (B) mouse (bar indicates 100μm) as well as 40X magnifications $TLR4^+$ (C) or a $TLR4^-$ (D) (bar indicates 10μm). Also shown are 10X images of Van Gieson (collagen) stained sections from a $TLR4^+$ (E) or a $TLR4^-$ (F) mouse (bar indicates 100μm). No noticeable differences in fibrous capsule formation were found between the two strains.

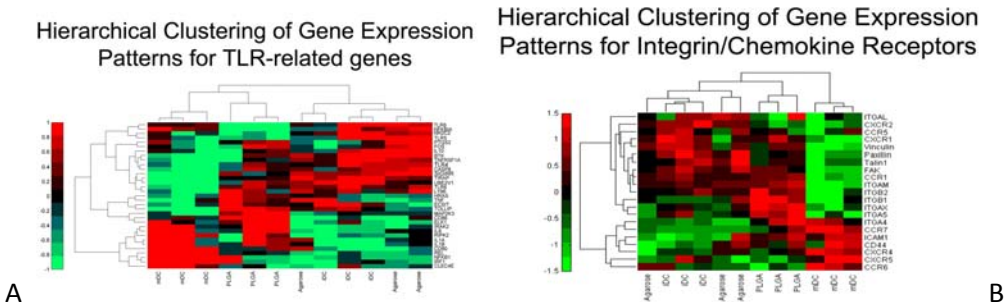

Figure 25: Hierarchical Clustering of Gene Expression Patterns for TLR-related Genes taken from RT^2 Profiler Array (TLR focused) (A) and for Integring and Chemokine Receptors (genes were chosen based on published human monocyted-derived DC integrin/chemokine receptor expression) (B). Genes analyzed/shown were found to be affected by at least one treatment by ANOVA analysis ($p<0.05$). Clustering was done using $-\Delta C_t$ values with a Pearson Distribution in Matlab.

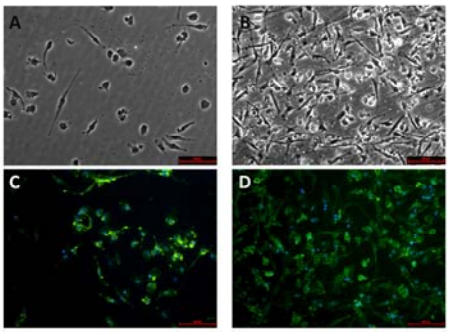

Figure 26: Adherent DC morphology on TCPS or PLGA films. DCs were cultured on TCPS (A,C) or treated with PLGA films (B,D) for 24h, stained with DC-SIGN-FITC and DAPI for nuclei visualization. Microscopy was performed at 20X. Representative of n=3 determinations. Scale bar denotes 100μm.

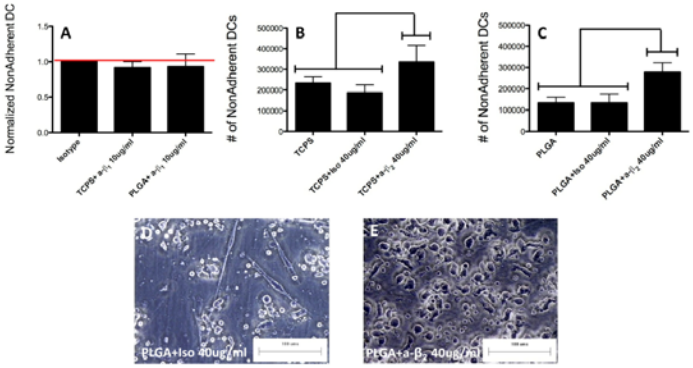

Figure 27: β_1 or β_2 integrin antibody blocking of DCs cultured on TCPS or treated with PLGA films for 24h. (A) Anti-β_1 (or isotype) at 10μg/mL treatment was performed and DCs were subsequently on cultured on TCPS or treated with PLGA films for 24h. Non/loosely adherent DCs were collected and counted and values were normalized to that of isotype control (n=2 independent determinations, mean+range). (B) DCs were cultured on TCPS for 24h following anti-β_2 (or isotype) at 10, 20 or 40μg/mL treatment. Non-adherent DCs were collected, counted and averaged. Star indicates statistical difference from respective isotype and TCPS control (ANOVA, $p<0.05$) (n=5 independent determinations, mean+s.d.) (C) DCs were cultured on PLGA for 24h following anti-β_2 (or isotype) at 10, 20 or 40μg/mL treatment. Non-adherent DCs were collected, counted and averaged. Star indicates statistical difference from respective isotype and PLGA control (ANOVA, $p<0.05$) (n=5 independent determinations, mean+s.d.) (D&E) Morphology of DCs cultured on PLGA following isotype (D) or anti-β_2 (E) treatment, representative of n=5 determinations. Scale bar denotes 100μm. Brackets in B and C denote statistical difference between groups (ANOVA, $p<0.05$).

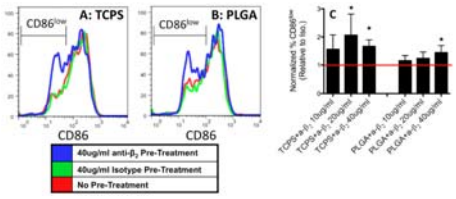

Figure 28: DC maturation marker (CD86) expression following anti-β_2 treatment. Representative (of n=5 determinations) flow cytometry results of DC CD86 expression at 24h treatment on TCPS (A) or PLGA (B) following pre-treatment of 40μg/mL of anti-β_2 (blue), isotype (green) or no treatment (red). $CD86^{low}$ gate for PLGA was double that of TCPS since PLGA induces increases in CD86 expression. (C) The percentage of DCs in $CD86^{low}$ gate was determined for each donor and normalized to that of isotype controls for each concentration examined. Star denotes statistical difference from isotype (1), Student T-test $p \leq 0.05$ (n=5 independent determinations, mean+s.d).

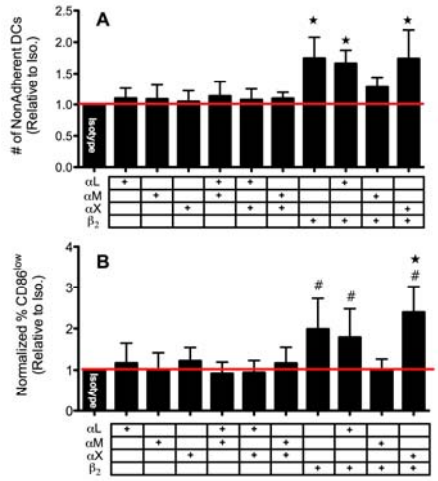

Figure 29: DC adhesion (A) and maturation (B) level following anti-$\alpha_L/\alpha_M/\alpha_X$ and/or anti-β_2 blocking on TCPS. A. Following anti-$\alpha_L/\alpha_M/\alpha_X$ blocking in combination with anti-β_2 (each at 20μg/mL) as denoted by table (+) under graph, non-adherent DC counts were collected. Values were normalized for each donor to that of isotype (1), n=8 independent determinations, mean+s.d. B. Following anti-$\alpha_L/\alpha_M/\alpha_X$ blocking in combination with anti-β_2 as denoted by table (+) under graph, the percentage of DCs in $CD86^{low}$ gate was determined by flow cytometry and normalized to that of isotype (n=6-8 independent determinations, mean+s.d). Stars for (A) & (B) denote statistical difference from all anti-α combination treatments (ANOVA, $p<0.05$). # designates statistical difference from isotype (1), Student T-test $p\leq0.05$.

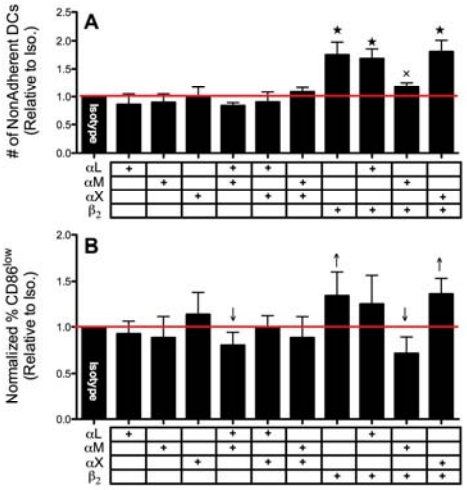

Figure 30: DC adhesion (A) and maturation (B) level following anti-$\alpha_L/\alpha_M/\alpha_X$ and/or anti-β_2 blocking data on PLGA. (A) Following anti-$\alpha_L/\alpha_M/\alpha_X$ blocking in combination with anti-β_2 (each at 20μg/mL) as denoted by table (+) under graph, non-adherent DC counts were collected. Values were normalized for each donor to that of isotype (1), n=5-6 independent determinations, mean+s.d. (B) Following anti-$\alpha_L/\alpha_M/\alpha_X$ blocking in combination with anti-β_2 as denoted by table (+) under graph, the percentage of DCs in $CD86^{low}$ gate was determined by flow cytometry and normalized to that of isotype (n=5-6 independent determinations, mean+s.d). Stars for (A) denote statistical difference from all lower values (ANOVA, $p<0.05$). X indicates statistical difference from anti-α_L + anti-α_M (ANOVA, $p<0.05$). Arrows for (B) indicates statistically above or below isotype (1), Student t-test $p\leq0.05$.

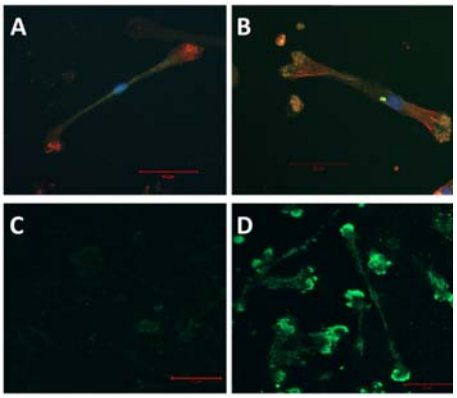

Figure 31: : β_1 vs. β_2 integrin expression on DCs adhering to PLGA films. DCs were allowed to adhere to PLGA films for 1.5h and subsequent were fixed, permeabilized and stained with either anti-β_1-FITC (A) or anti-β_2-FITC (B) both in combination with phalloidin-TRITC (red) and nuclei (green). To examine receptors at DC-biomaterial interface alone, DCs were treated with PLGA films for 1.5h and cross-linked to surface using DTSSP. Non-cross-linked components were then extracted using 0.1% SDS. Polyclonal antibodies (goat) against β_1 (C) or β_2 (D) were used in combination with anti-goat-FITC secondary to detect integrin presence remaining on films. All films were imaged using confocal microscopy at 40X. Scale bar denotes 50μm. Representative of n=3 determinations.

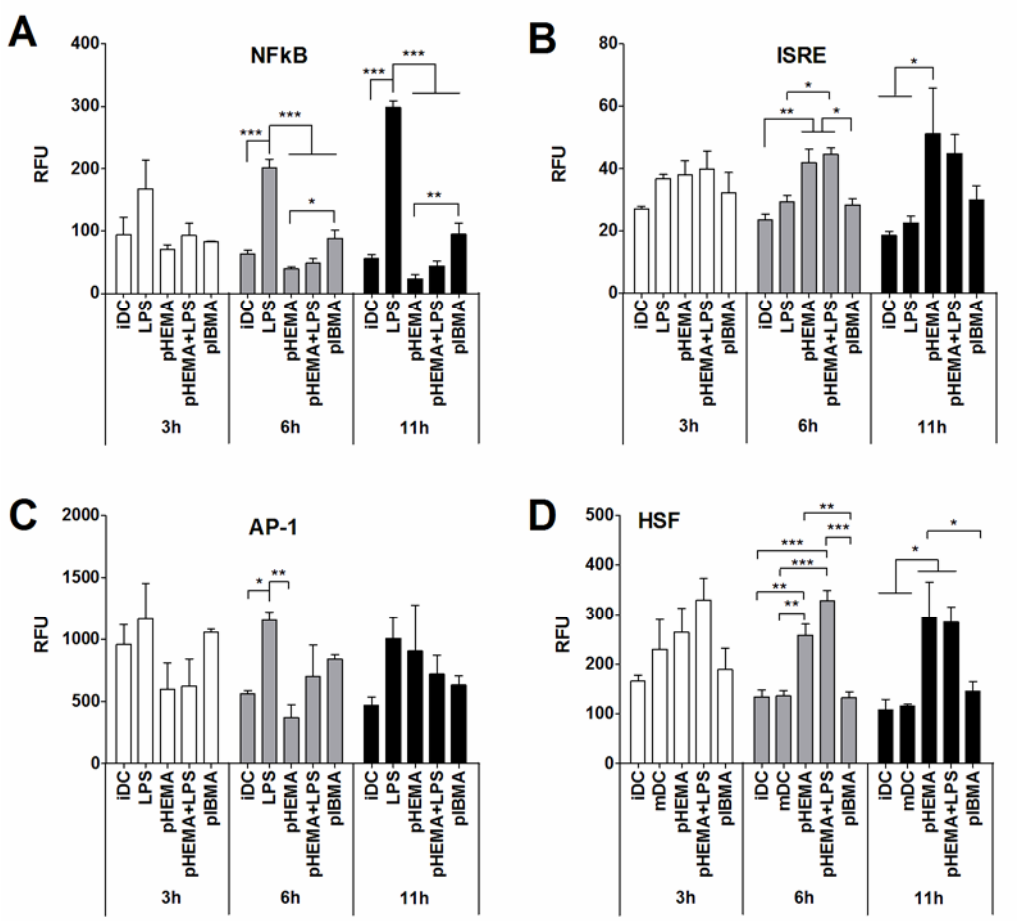

Figure 32: Transcription factor profiles induced by differentially treated DCs. These TFs have been previously shown to support or associated with DC maturation. *: p<0.5, **:p<0.01, ***: p<0.001

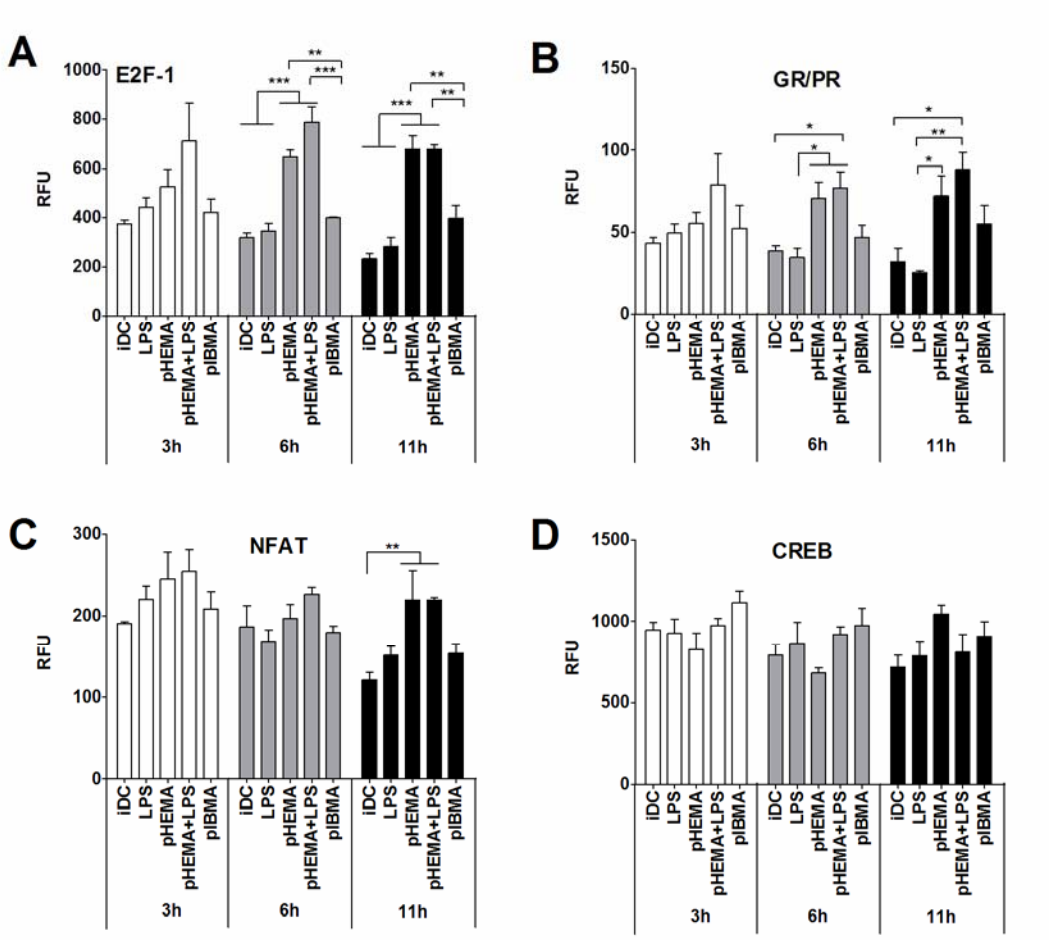

Figure 33: Transcription factor profiles induced by differentially treated DCs. E2F-1 and GRE/PR have been previously shown to suppress DC maturation. NFAT has been shown to maintain DCs in the immature stage. GREB has been shown to prevent DCs from apoptosis. *: p<0.5, **:p<0.01, ***: p<0.001

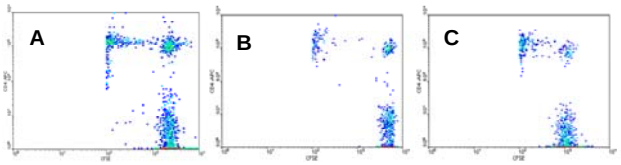

Figure 34: **:** Proliferation of adoptively transferred OT-II T cells 3 days following antigen carrier vehicle challenge, CFSE and CD4 fluorescence on x- and y-axes, respectively. C57BL/6 mice challenged with 1 mg/ml OVA co-delivered with (A) CFA,

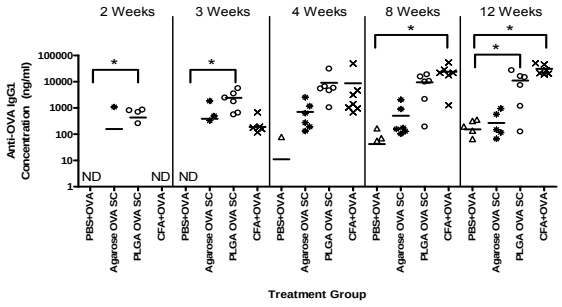

Figure 35: Sera concentrations of anti-OVA IgG1 antibodies for C57BL/6 mice treated OVA delivered in PBS, from agarose or PLGA scaffolds or delivered in CFA (n = 6-7). Individual mouse data are shown with mean represented as a line. *: $p<0.05$ by ANOVA with Dunnett's post-test. ND = not detectable.